

# Vortex Molecules in Spinor Condensates

Ari M. Turner\*<sup>†</sup> and Eugene Demler\*

\**Department of Physics, Harvard University, Cambridge MA 02138 and*

*†Department of Physics, University of California, Berkeley CA 94720*

(Dated: November 21, 2018)

Condensates of atoms with spins can have vortices of several types; these are related to the symmetry group of the atoms' ground state. We discuss how, when a condensate is placed in a small magnetic field that breaks the spin symmetry, these vortices may form bound states. Using symmetry classification of vortex-charge and rough estimates for vortex interactions, one can show that some configurations that are stable at zero temperature can decay at finite temperatures by crossing over energy barriers. Our focus is cyclic spin 2 condensates, which have tetrahedral symmetry.

In an image of a nematic liquid crystal by polarized light, one can identify topological defects of various topological charges (see Ref. [1]). Bose condensates (see the books[2, 3]) are starting to provide another context for studying topological defects: in the texture formed by the phase *and* spin of a spinor condensate[4, 5, 6]. (See also [7, 8] for reviews of the theory and experimental techniques being applied to spinor condensates.)

A topological defect in the *phase of a superfluid* is a quantized vortex. The discontinuity in the phase as the defect is encircled must be  $2\pi n$  for an integer  $n$ , and the circulation of the vortex is then  $n\frac{h}{m}$ . In a single-component superfluid, multiply quantized vortices ( $|n| > 1$ ) are usually not stable. The widely known explanation is that the energy of a vortex is proportional to  $n^2$ . Thus a doubly quantized vortex ( $n^2 = 4$ ) can lower its energy by splitting into two singly quantized vortices. Similar arguments can be formulated for multicomponent condensates, but we will find that some vortices in these condensates can be very long-lived in spite of having large energies. Our predictions are about condensates of atoms with spin in which the rotational symmetry has been weakly disrupted by a small parameter  $q$ , such as the interaction between the spins and the magnetic field. (We focus on the *cyclic* condensates of spin 2 atoms, see Ref. [9].)

Long-lived multiply quantized vortices are particular examples of composite vortices, which are made up of several vortices bound together. Ground states with complicated symmetries have many types of vortices[10]. Symmetry violating fields provide a force that can bind some groups types vortices together so that they form a “composite core” for a larger vortex. The composite vortex might have two quanta of circulation (or have some other extra-large topological charge). Such a vortex would be surprising if observed under a low resolution, because the smaller vortices that make it up would be hidden in its core; the behavior of the order parameter at infinity is determined entirely by the *net* topological charge.

Some earlier theories about vortices in multicomponent condensates also describe vortices with asymmetrical cores which can be regarded as collections of closely spaced vortices. The parameter  $q$  makes this interpretation even more meaningful: when  $q$  is very small, we find

that the component vortices move far apart, so that their cores do not overlap, while still remaining bound. Ref. [11] describes vortices that can occur in a condensate of two atomic states when there is an RF-field producing coherent transitions between the states. The binding of these vortices also comes from an asymmetry, but the asymmetry comes from the dependence of the interaction strength on the internal states of the atoms, rather than from an external magnetic field. Ref. [12] studies vortices of spinor atoms in a magnetic field, like us, but focuses on spin 1, and describes composite vortices as well. Since the scenario involves rotation as well as a magnetic field, the vortices would be held close to the *axis* of the condensate by rotational confinement without the magnetic field. With just a magnetic field, we show that the vortices are attracted to *one another*.

Vortices and bound states are not hard to picture, by taking advantage of the fact that the state of a spinor atom can be represented by a geometrical figure. The appropriate shape depends on the type of condensate. For a ferromagnetic condensate, a stake pointing in the direction of the magnetization could represent the local state of the condensate. Other condensates can be represented by more complicated shapes. Now imagine a plane filled with identical shapes (tetrahedra, for the cyclic phase), with orientations varying continuously as a function of position. This shape field (or “spin texture”) together with a phase field would represent a nonuniform state of a condensate. If the shapes rotate around a fixed symmetry axis as some point is encircled then the spin texture has a topological defect at this point. Such configurations generalize vortices, because some of them are accompanied by persistent spin or charge currents. For each symmetry of the tetrahedron, there will be a vortex when the Hamiltonian is  $SU_2$  symmetric. (Each discrete subgroup of  $SU_2$  describes the vortices of some phase for atoms of some spin[13]; to find vortices for more even more complicated groups like  $SO_5$  or  $SO_7$ , one might want to study gases of spin  $\frac{3}{2}$  atoms[14, 15].) The vortex spectrum is decimated when a magnetic field is applied, since the field favors a particular orientation of the order parameter –e.g., tetrahedra may want to have an order-three axis aligned with the magnetic field. The spectrum of vortices is then reduced from the full spectrum of “tetrahedral” vortices (based on arbitrary symmetries

of the tetrahedron) to “field-aligned” vortices, where the tetrahedra must rotate around this order three axis, so as not to lose their alignment with the magnetic field. We may introduce the ground state space  $\mathcal{M}_q$  (of tetrahedra aligned with the magnetic field), where the interaction energy is  $V = V_{min}$ , and the space of ground states of the  $SU_2$  invariant part of the Hamiltonian,  $\mathcal{M}$  (of tetrahedra with arbitrary orientations). A set of vortices can be assigned a topological charge based on the loop traced out in one of these spaces by the values of the order parameter on a circle around the set. Specifically, the topological charge describes the symmetry transformation that brings the order parameter back to its initial value as the set of vortices is circumambulated. (The relation between topology and symmetry is presented in [10].) From the general point of view, the reduction of the charge types from the tetrahedral to the field-aligned ones when  $q$  is turned on results because the smaller ground state space at nonzero  $q$ ,  $\mathcal{M}_q$ , has fewer closed loops[52].

If  $q$  is very small, the excess energy of an order parameter in  $\mathcal{M}$  rather than  $\mathcal{M}_q$  is small. There is then a hierarchy of spaces  $\mathcal{M}_q$ ,  $\mathcal{M}$  and  $\mathcal{H}$  (the whole Hilbert space, corresponding to arbitrarily *distorted* tetrahedra) with increasing energy scales. When  $q \neq 0$ , a vortex has to have a field-aligned charge *at infinity* because the tetrahedra must eventually move into  $\mathcal{M}_q$  to avoid too big of an energy cost. But if  $q$  is small, the hierarchy of the order parameter space is reflected in the fact that a vortex with a field-aligned charge can have a *composite* core that may contain tetrahedral vortices, as in Fig. 1; the core is sort of like the pulp and seeds of a fruit. Inside the fruit is a texture of arbitrarily oriented tetrahedra, almost as if  $q$  were equal to zero. The seeds are then the cores of tetrahedral vortices and the pulp is qualitatively the same as the texture that would surround these vortices in the absence of the magnetic field. The net charge of the vortices has to be field-aligned so that the loop of order parameters that surrounds the whole core can move into  $\mathcal{M}_q$  as  $r \rightarrow \infty$ . This picture becomes more accurate as  $q$  becomes small, since the vortex cores within the composite core are far apart in that case—the size of a region where the order parameter is in  $\mathcal{M} - \mathcal{M}_q$  or  $\mathcal{H} - \mathcal{M}$  is inversely proportional to the energy scale for each space. As  $q \rightarrow 0$ , the binding of the tetrahedral charges becomes weaker and weaker, until they become free from each other; each vortex therefore is described by independent degrees of freedom when  $q = 0$ .

The optimal size  $L_q$  of a composite vortex results from competition between two forces—a confinement force from the anisotropy term and the familiar logarithmic interaction of vortices. The symmetry breaking energy favors minimizing the area over which the order parameter leaves  $\mathcal{M}_q$ , pushing the component vortices toward one another. On the other hand, it cannot compress them to a point since the Coulomb-like repulsion one expects of vortices keeps them apart.

Some of these vortex molecules will turn out to be metastable. Ref. [12] mentions an interesting clue to

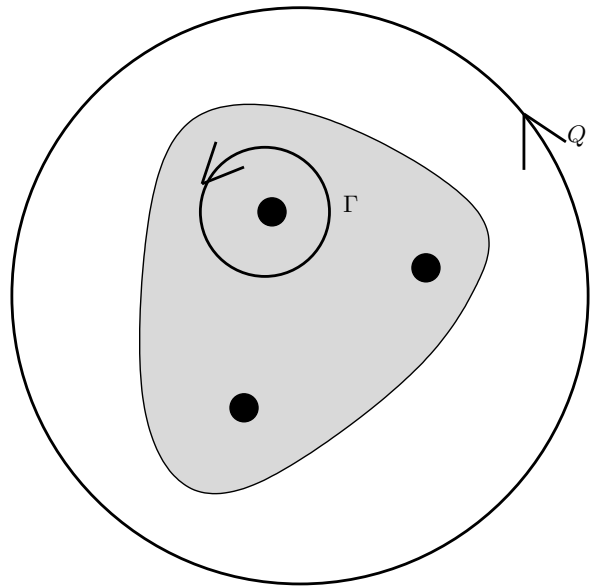


FIG. 1: A composite vortex reflects the hierarchy of the order parameter space. In the white, grey, and black regions the order parameter moves from  $\mathcal{M}_q$  to  $\mathcal{M}$  to  $\mathcal{H}$  which has the highest energy of all. The charges of the subvortices are tetrahedral charges, represented by  $\Gamma$  and the charges of the composite vortex is a “field-aligned” charge.

such a phenomenon; namely there are multiple steady state wave functions describing a condensate with a given magnetization and rotational frequency; these local minima of the energy function can maybe be analyzed using the group theoretic metastability conditions we discuss in Section III C. For a spinor condensate, wave functions for states besides the ground state are experimentally important, since the experiments of Ref. [16], as well as the liquid crystal experiments of Ref. [17], reveal complicated textures produced by chance; an initial fluctuation around a uniform excited state becomes unstable and evolves into an intricate *nonequilibrium* texture. So it is useful to analyze spin textures which are only *local* minima of the Gross-Pitaevskii energy functional (like the metastable vortex molecules considered here) as well as unstable equilibria (which take a long time to fluctuate out of their initial configuration). Examples of unstable equilibrium are described for single-component condensates by [18]. The process by which textures form out of uniform initial states has been discussed in theoretical articles, including [19, 20] (on the statistics of the spin fluctuations and vortices that are produced from this random evolution), [21] (on the spectrum of instabilities) and [22, 23] on the dynamics of spinor condensates. The experiments described in [24] show that the patterns that evolve in rubidium condensates are probably affected by dipole-dipole interactions, though we are not considering these. Dipole-dipole interactions lead to antiferromagnetic phases[25], which maybe can be described as *ground state* configurations of vortices.

Besides just hoping for unusual types of vortices to

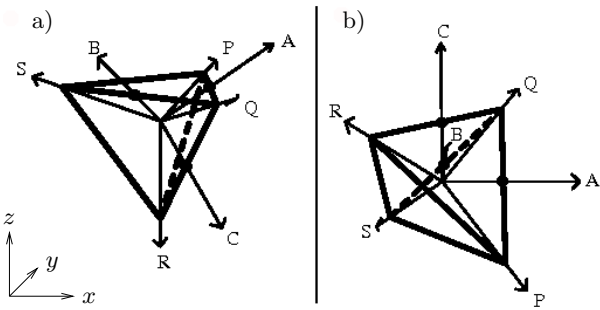


FIG. 2: Geometrical representation of the tetrahedral superfluid phases of spin 2 atoms. Two orientations of a tetrahedron, corresponding to the spin roots of the ground state spinor, are illustrated and the symmetry axes are labelled. (The orientation of the coordinate axes, shown on the side, is the same in both cases.) a) An orientation with the vertical  $z$ -axis along an order three axis, corresponding to the ground state  $\sqrt{n_0}\chi_3$  (see Eq. (2)). b) An orientation with the  $z$ -axis along an order two axis, corresponding to the ground state  $\sqrt{n_0}\chi_2$  (see Eq. (29)). For a magnetic field along the  $z$  axis, orientation a) is preferred when  $c > 4$  and orientation b) is preferred when  $c < 4$ . Note that the three order 2 axes, labelled  $A, B, C$  can be used as a set of three orthogonal body axes.

form, one can make a vortex lattice by rotating a condensate. The effects of rotating on a spinor condensate have been investigated theoretically in [26] as well as the review [27]. Experiments can also make a single vortex of a prescribed type[28, 29, 30]. Excited by these possibilities, physicists have come up with several types of vortices and topological defects they would be interested in seeing: skyrmions[31, 32], monopoles[33], textures whose order parameter-field lines make linked loops[34], as well as the noncommutative vortices of the cyclic phase that we will be expanding on here[35].

The key to our discussion of vortices will be a geometrical representation of the order parameter, allowing us to visualize a texture of the cyclic phase as a field of tetrahedra with different orientations. (See Fig. 2.) Without this representation, a spin texture would be given by a spinor field  $(\psi_2(x, y), \psi_1(x, y), \psi_0(x, y), \psi_{-1}(x, y), \psi_{-2}(x, y))^T$ ; the fact that this spinor lies in the ground state manifold  $\mathcal{M}$  would have to be described by a set of polynomial relations between the five components. A more revealing way to represent a spinor is to draw a geometrical figure consisting of “spin-roots” (as in [36]), and in the cyclic phase, these spin roots form the vertices of a tetrahedron. (A similar construction can be used to classify vortices in condensates of spin 3 atoms, see Ref. [37].) Even without using the spin-root interpretation, one can justify using tetrahedra to represent order parameters in the cyclic phase because they are a concrete way of rep-

resenting the symmetry of this phase. Ref. [35] worked out the symmetry group of a state in the cyclic phase by finding all the pairs  $\hat{\mathbf{n}}, \alpha$  such that

$$e^{-i\alpha\mathbf{F}\cdot\hat{\mathbf{n}}}\chi_3 \propto \chi_3 \quad (1)$$

where

$$\chi_3 = \begin{pmatrix} \sqrt{\frac{1}{3}} \\ 0 \\ 0 \\ \sqrt{\frac{2}{3}} \\ 0 \end{pmatrix}. \quad (2)$$

The spinor  $\sqrt{n_0}\chi_3$  is a representative cyclic state, if  $n_0$  is the density of the condensate. These symmetries are the same as the symmetries of a tetrahedron oriented as in Fig. 2a; hence we may represent the state  $\sqrt{n_0}\chi_3$  by this tetrahedron. Any other ground state should be represented by a tetrahedron oriented so that its symmetry axes and symmetry axes of the spinor coincide. The appropriate orientation of the tetrahedron for a given ground state can be determined in an automatic way by calculating the spin roots.

The Hamiltonian for spin 2 atoms in a magnetic field,  $\mathcal{H} = \iint d^2\mathbf{u}[\frac{\hbar^2}{2m}\nabla\psi^\dagger\nabla\psi + V_{tot}(\psi)]$  has a simple expression[9] in terms of the density  $n = \psi^\dagger\psi$ , magnetization  $\mathbf{m} = \psi^\dagger\mathbf{F}\psi$ , and singlet-pair amplitude  $\theta = \psi_t^\dagger\psi$ . ( $\psi_t$  stands for the time reversal of  $\psi$ .)

$$V_{tot}(\psi) = \frac{1}{2}(\alpha n^2 + \beta\mathbf{m}^2 + c\beta|\theta|^2) - q\psi^\dagger F_z^2\psi - \mu\psi^\dagger\psi \quad (3)$$

The first three terms describe the rotationally symmetric interactions of pairs of atoms. The first one describes repulsion between a pair of atoms and the next two terms describe additional, smaller interactions, that depend on the spin states of the two colliding atoms. These terms determine the spinor ground state in the absence of a magnetic field[9]. (The spin-dependent interaction strengths  $\beta, c\beta$  can be expressed in terms of the scattering lengths.) The properties of spin 2 atoms, which are described by this Hamiltonian, and of spin 1 atoms have been investigated experimentally in Refs. [16, 38, 39, 40, 41]; [42] reviews more experimental phenomena. Ref. [39, 40] found values for  $\alpha, \beta$  and  $c$  for  $^{87}\text{Rb}$  that are consistent with theoretical predictions, although even the sign of  $c$  is not known for sure, because  $c$  is small. The final term contains the chemical potential  $\mu$ .

If  $\beta$  and  $c$  are positive, the ground state of a condensate of spin 2 atoms is cyclic. The deformation of a cyclic state due to a magnetic field is the simplest if we assume that  $\alpha \gg |\beta|$  and that  $c$  is on the order of 1. We therefore assume  $c \sim 1$ , though  $c \ll 1$  for rubidium. The magnetic field influences the atoms through the fourth term of the energy, breaking the rotational symmetry of the Hamiltonian; this term describes the quadratic Zeeman shift due to a magnetic field  $B$  along the  $z$ -axis

and  $q \propto B^2$ . (See [2] for the explanation of why the quadratic Zeeman term  $q$  but not the linear term is relevant if the condensate's initial magnetization is zero. A nonzero magnetization is described by a Lagrange multiplier term  $-p \iint d^2\mathbf{x} \psi^\dagger F_z \psi$ , which looks like a linear Zeeman coupling. We assume  $p = 0$ ; a nonzero  $p$  should have similar consequences as a nonzero  $q$ , since both break the rotational symmetry.)

Introducing a small  $q$  reduces the ground state space from  $\mathcal{M}$  to  $\mathcal{M}_q$ . This can be explained (see Sec. II A) by finding the modulation of the energy of an arbitrary tetrahedral state as a function of the orientation of the corresponding tetrahedron:

$$V_{eff} = (c - 4) \frac{3q^2}{4c\beta} (\cos^4 \alpha_1 + \cos^4 \alpha_2 + \cos^4 \alpha_3), \quad (4)$$

where  $\alpha_1, \alpha_2$  and  $\alpha_3$  are the angles between the  $z$ -axis and three body-axes  $A, B, C$  fixed to the tetrahedron (see Fig. 2a). The orientations that minimize this energy are the true ground states at nonzero  $q$ . If  $c > 4$  (assumed until Sec. IV), then the tetrahedron in its ground state is oriented with the  $z$ -axis perpendicular to a face as in Fig. 2a, with a ground state energy of  $V_{min} = \frac{(c-4)q^2}{4c\beta}$ . Thus the absolute ground state space  $\mathcal{M}_q = \mathcal{M}_{q3}$  contains all the wave functions that are arbitrary rotations about the  $z$ -axis (combined with rephasings) of  $\sqrt{n_0}\chi_3$ . When  $c < 4$ , the ground states  $\mathcal{M}_{q2}$  are rotations about  $z$  of the tetrahedron illustrated in Fig. 2b. In particular, when  $q \neq 0$ , there is a phase transition at  $c = 4$ , though there is nothing special about  $c = 4$  in *zero* magnetic field. In this paper, we will mostly assume that  $c > 4$  because our initial example occurs under this condition.

Consider first a single vortex associated with the rotation through  $180^\circ$  of the ground state tetrahedron (see Fig. 2a) about the  $A$  axis,  $(\sqrt{\frac{2}{3}}, 0, \sqrt{\frac{1}{3}})$ . Such a vortex is described at large distances by

$$\psi(r, \phi) = e^{-i\frac{\phi}{2}} \frac{1}{\sqrt{3}} (\sqrt{2}F_x + F_z) \sqrt{n_0}\chi_3 \quad (5)$$

where  $r, \phi$  are polar coordinates centered on the core of the vortex. This vortex has an excess energy (relative to the ground state energy of the condensate) which diverges with the condensate size. In fact, its Zeeman energy density (with  $V_{min}$  subtracted) is given according to Eq. (4) by [53]

$$\frac{(c-4)(q^2)}{6\beta c} (\sin^2 \phi). \quad (6)$$

The tetrahedron is pointing in the wrong direction except along the positive and negative  $x$ -axis; and the integrated energy is proportional to the area:

$$E_{misalign} \sim \frac{q^2 R^2}{\beta c} \quad (7)$$

where  $R$  is the condensate's radius. Such a vortex cannot be the only vortex in an infinite condensate!

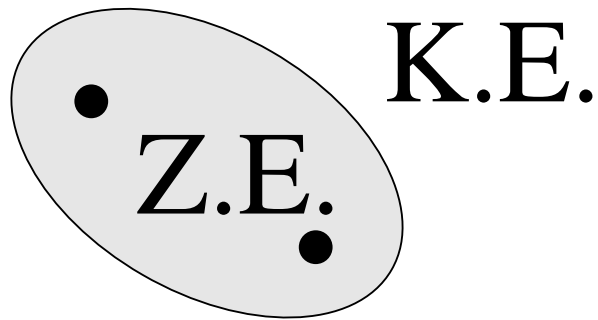


FIG. 3: Illustration of the energy costs in a vortex molecule. The energy in the region occupied by the two vortices is dominated by the quadratic Zeeman cost and the energy outside it is dominated by kinetic energy. Increasing the molecule size decreases the kinetic energy and increases the Zeeman energy. The equilibrium size  $L$  is determined by minimizing the sum.

The vortex described by Eq. (5) can form a partnership with another vortex of the same type, producing a molecule that can exist without costing too much energy. This is because the net charge of the two vortices is compatible with the magnetic field. The combination of two  $180^\circ$  rotations of the tetrahedral order parameter about the  $A$  axis is a  $360^\circ$  rotation about the  $A$ -axis, but since any rotation axis is a  $360^\circ$  symmetry of the tetrahedron, the rotation axis on circles of radius  $r$  enclosing the vortices can be tilted continuously relative to the tetrahedron as  $r$  increases until it becomes the  $R$  axis instead. Then the tetrahedra align with the magnetic field far from the vortices and stay in  $\mathcal{M}_{q3}$ . Each vortex screens the part of the other vortex's charge that produces the large Zeeman cost, as illustrated in Fig. 3. The Zeeman energy in the region around the vortices, where the tetrahedra are still tilted, may be estimated by replacing the total condensate size  $R$  in Eq. (7) by the diameter  $L$  of this region. The Zeeman energy tries to pull the vortices toward one another but the elastic energy cost of rapid changes in the order parameter (the gradient term in the Hamiltonian) opposes this tendency: The tetrahedra rotate twice as fast around circles beyond  $L$ , where the two vortices act in concert. Therefore the elastic energy increases as  $L$  becomes smaller; this leads to the Coulomb repulsion between the vortices,  $2\pi \frac{n_0 \hbar^2}{m} \ln \frac{R}{a} - \pi \frac{n_0 \hbar^2}{m} \ln \frac{L}{a_c}$ , where  $m$  is the mass of the atoms in the condensate. The energy of the vortex molecule is therefore

$$E = k \frac{q^2 L^2}{\beta} - \pi \frac{n_0 \hbar^2}{m} \ln \frac{L}{a_c} + cns. \quad (8)$$

where  $k$  is a numerical constant. The equilibrium size can be determined by minimizing over  $L$ . The quadratic Zeeman force binds this molecule together while the repulsion keeps the vortices from merging.

If the vortices *were* to coalesce, then they could react to form a set of vortices that are not bound by the Zeeman energy; one possible set of decay products is three vortices each involving a rotation through  $120^\circ$  about

the  $R$  axis (which have the same net  $360^\circ$  rotation as the original pair of vortices). The vortex molecule of the two  $A$  rotations is *metastable* because thermal fluctuations may overcome their Coulomb repulsion and push them together, leading to such a fission process.

The rest of this paper elaborates: it gives a qualitatively correct expression for the spin texture surrounding the molecule just described and determines how this molecule *actually* decays. In order to do this, we will give some more general results: first Section I, summarizes the non-commutative group theory of combining vortex charges and a classification of the tetrahedral vortices (the vortices that occur by themselves when  $q = 0$  and in clusters when  $q \neq 0$ ); then Section II estimates the elastic energies and Zeeman energies of such clusters as functions of these vortex charges; finally Section III gives criteria determining which types of tetrahedral vortices form bound states or metastable states (see Section III C). The last two sections illustrate the criteria with a few additional surprising examples (see Section IV) and give some basic ideas about how to observe metastable vortices (Section V).

## I. TOPOLOGICAL CHARGES

Vortices are simplest to understand for an interaction energy that has a single manifold,  $\mathcal{N}$ , of ground states and no hierarchy. The order parameter must move into  $\mathcal{N}$  far away from any spin texture. Vortices are classified by the topology of the circuit traced out in  $\mathcal{N}$  by the order parameter on a large circle containing a vortex or set of vortices. Although there are many ways to add wiggles to a given circuit, only the topological structure is important, leading to a discrete set of possible vortex charges. Fig. 4 shows how a circuit may be tangled with holes in the space  $\mathcal{N}$ . As a vortex evolves, such a circuit can evolve only into other circuits that are tangled in the same way; thus the vortex charge is conserved.

This generalizes circulation-conservation in a single-component condensate: The circulation quantum number  $n$  for a set of vortices is also the number of times that the wave function at infinity winds around the circle that minimizes the Mexican hat potential[43]. The tangling in a multicomponent condensate can be described by a group of generalized winding numbers around the ground state manifold  $\mathcal{N}$ ,  $\pi_1(\mathcal{N})$ , the “fundamental group” (see Fig. 4).

Besides the conservation of topological charge, two further properties of vortices follow from the geometry of the internal ground-state space. First of all, the *net winding* or topological “charge” of a set of vortices can be found by multiplying their charges together, using the definition of multiplication for the fundamental group. (In a general space, the fundamental group has a multiplication operation defined by splicing circuits together.) This rule is the generalization of adding the  $n$ ’s of the individual vortices in the scalar order-parameter case. (The funda-

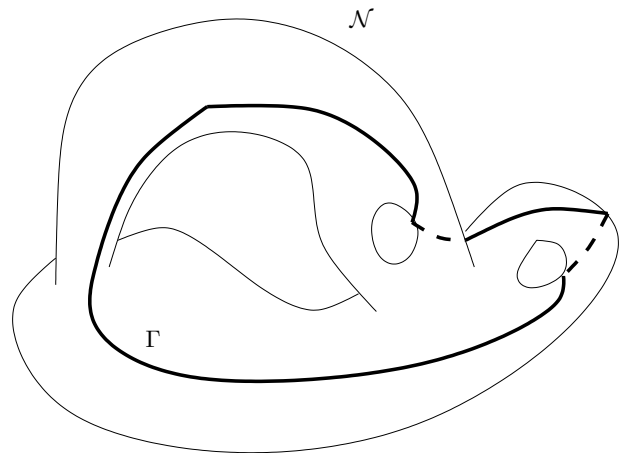


FIG. 4: The order parameter at infinity of a vortex winds around a loop  $\Gamma$  in the order parameter space  $\mathcal{M}$ . Realistic order parameter spaces are usually more symmetrical.

mental group is noncommutative so one has to multiply the charges together in the right order, see Appendix B.)

Secondly, the *energy* of a vortex can be estimated as a function of the winding behavior at infinity. For a vortex that *minimizes* this energy, the order parameter travels along a geodesic in  $\mathcal{N}$ . Since the interaction energy  $V$  is constant (and equal to its minimum  $V_{min}$ ) at infinity, the energy of a vortex is determined by the elastic energy, that is, the cost of variations in  $\psi$  as a function of the azimuthal angle  $\phi$ . The closed loop traced out by  $\psi(R \cos \phi, R \sin \phi)$  will relax to make this energy-cost small. When it shrinks as much as is possible without leaving  $\mathcal{N}$ , it becomes a *geodesic* in  $\mathcal{N}$ . The energy of the vortex is related to the length  $l$  of this geodesic by

$$E = \left( \frac{\hbar^2 n_0}{m} \ln \frac{R}{a_c} \right) \frac{l^2}{4\pi} \quad (9)$$

where  $R$  and  $a_c$  are the radii of the condensate and the vortex core. (Note that replacing  $l$  by  $2\pi n$  gives the standard expression for a vortex in a scalar condensate.)

A small magnetic field introduces hierarchies into the order parameter space, leading to spin textures that wind around one manifold at an intermediate length scale and around a smaller manifold far away.

### A. Spin Textures and their Vortices

Let us consider how nested vortices hold themselves together in a continuous “spin texture.” We will try to give a general argument showing how topology and the energy-hierarchy of the order parameter spaces implies that any texture is made up of a set of composite vortices which in turn are made up of clusters of nearly point-like vortices.

The order parameter subspaces in order of increasing energies are the two-dimensional  $\mathcal{M}_q$ , the four-dimensional  $\mathcal{M}$  and the  $4F + 2$  dimensional  $\mathcal{H}$  (for

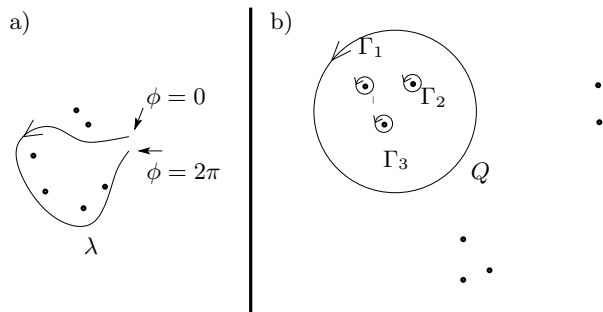


FIG. 5: Classifying vortex topologies. a) The combined topology of a set of vortices can be found by seeing how the order parameter changes around a closed loop parameterized by  $\phi$ . The loop is drawn with a small gap between  $\phi = 0$  and  $\phi = 2\pi$  to indicate that  $g(\phi)$  and  $\theta(\phi)$  vary continuously only between 0 and  $2\pi$ . The topological charge is defined as the jump in the values of  $g$  and  $\theta$  across the gap. b) Vortices that cannot exist by themselves in the presence of a magnetic field can still sometimes appear in clusters. The charges  $\Gamma_1, \Gamma_2, \Gamma_3$  in one of the clusters can involve rotations around arbitrary axes, but the combined charge  $Q$  has to use the direction of the magnetic field for its rotational axis to avoid a large energy-cost.

spin  $F$ ), with corresponding energy scales  $V - V_{min} = 0$ ,  $\epsilon(q) = \frac{q^2}{\beta}$  (see Eq. (4)) and  $\beta n_0^2$  (see Eq. (3)); as long as the density of the condensate does not vary,  $\beta$  rather than  $\alpha$  sets the energy scale). The condensate can move out of the ground state into one of the higher-energy subspaces if forced to by topology, spending less space in the manifolds with the greater energies. (This is like saving eggnog—with all that fat!—for one week out of the year.) For a particular subspace  $\mathcal{M}_i$  in this sequence, in which  $V(\psi) - V_{min} \sim \epsilon_i$ , the size  $L_i$  of the regions where  $\psi$  is in  $\mathcal{M}_i$  is typically  $L_i \sim \sqrt{\frac{K}{\epsilon_i}}$ , where  $K = \frac{\hbar^2 n_0}{m}$  is the elasticity of the condensate. This relation can be guessed at without understanding anything about the field configuration in such a region; just assume equipartition between kinetic and interaction energies, so that  $\epsilon_i$  is equal to  $\frac{K}{L_i^2}$ , a typical scale for the kinetic energy density,  $\frac{\hbar^2}{2m} |\nabla\psi|^2$ . Consequently, the composite vortex cores in Fig. 1, where  $\psi$  is in  $\mathcal{M} - \mathcal{M}_q$ , have diameters

$$L_q \sim \sqrt{\frac{K\beta}{q^2}} \sim \frac{\hbar}{q} \sqrt{\frac{n_0\beta}{m}} \quad (10)$$

where the energy scale is taken from Eq. (4) and the component cores, where  $\psi$  varies through  $\mathcal{H} - \mathcal{M}$ , have typical diameters  $a_c \sim \sqrt{\frac{K}{n_0^2\beta}}$ .

The more complete version of the equipartition argument, given in Sec. IIIB, estimates the total energy of the vortex as follows: the kinetic energy outside the composite core is about  $K \frac{L^2}{4\pi} \ln \frac{R}{L}$ , according to Eq. (9), the magnetic field energy inside the core is about  $\epsilon(q)L^2$ . Minimizing the sum, which has the form  $-c_1 K \ln L + \epsilon(q)L^2 + c_2$ , gives  $L \sim \sqrt{\frac{K}{\epsilon(q)}}$ . The analogous

argument also applies to vortices in a single-component condensate, giving the core size  $\sqrt{\frac{K}{n_0^2\alpha}}$ . Because the composite cores in a cyclic condensate have some substructure (the component vortices), the actual coefficient  $c_1$  of the logarithm for the cyclic condensate will turn out to be less than  $\frac{1^2}{4\pi}$  once the kinetic energy of the vortices inside the core is included (see Section II B).

If  $q$  is very small, the component cores are much smaller than the composite vortices, and may be regarded as points. The wave function can therefore be approximated by a field that always stays in  $\mathcal{M}$  except at “singularities” corresponding to the component cores:

$$\psi(x, y) \approx e^{-i\alpha(x, y)\hat{\mathbf{n}}(x, y) \cdot \mathbf{F}} e^{i\theta(x, y)} \sqrt{n_0} \chi_3 \quad \text{except at “points”,} \quad (11)$$

where  $\chi_3$  is the spinor defined in Eq. (2). Over distances much greater than  $L_q$  even the composite cores seem to dwindle to points, suggesting the following approximation:

$$\psi(x, y) \approx e^{-i\alpha(x, y)F_z} e^{i\theta(x, y)} \sqrt{n_0} \chi_3 \quad \text{far from clusters.} \quad (12)$$

These expressions generalize[44] the “phase-only approximation” for ordinary superfluids[43]; for example, Eq. (11) parameterizes elements of the space  $\mathcal{M}$  in terms of the symmetries of the  $q = 0$  Hamiltonian, rotations  $\psi \rightarrow e^{-i\alpha\mathbf{F} \cdot \hat{\mathbf{n}}}\psi$ , and rephasings,  $\psi \rightarrow e^{i\theta}\psi$ , which are applied to a representative state. Vortices are points which look like singularities at the level of resolution exposed by one of these approximations, although what one identifies as vortex singularity depends on which level of resolution one uses!

Composite vortices result from the order parameter being forced out of the minimum-energy space  $\mathcal{M}_q$  by topology: If the order parameter goes around a hole in  $\mathcal{M}_q$  on some circle in the condensate, then inside the circle, the order parameter has to leave  $\mathcal{M}_q$ . If Eq. (12) continued to hold all the way to the center of the circle, then there would be a singularity since the angular variables  $\alpha$  and  $\theta$  would run rapidly through multiples of  $2\pi$ . So we can think of the circle as the core of an extended vortex in the field in Eq. (12). The singularity is actually filled in by a field of tetrahedra with higher-energy orientations, described by Eq. (11), just as the wave function of a vortex in a single-component condensate avoids singularities by vanishing in the core. In the filled-in region of freely-oriented tetrahedra, there are also some elementary “point”-vortices, actually spread out over the distance  $a_c$ . These result when the order parameter gets tangled around holes in  $\mathcal{M}$ , and then has to move outside of *this* space. These cores are smaller than the composite core because of the large energy scale associated with  $\mathcal{M}$ . The fields of these vortices can be described qualitatively by setting  $q = 0$  since kinetic energy surpasses the anisotropy energy very close to the cores.

The cores of the component vortices are filled to almost the same density  $n_0$  as the rest of the condensate

(the spin-independent repulsion  $\alpha$  favors uniformity since  $\alpha \gg \beta$ ). Vortices with this property are often referred to as “coreless,” but we use the word “core” in a more general way, so that every vortex can have one. Instead of defining core as a region where the *density* vanishes, our definition identifies a core as a region where the wave function departs from any particular form. (In the core of a “coreless” vortex in a ferromagnetic condensate, the order parameter becomes polar rather than ferromagnetic.) The core of the component tetrahedral vortices is the region where the order parameter leaves  $\mathcal{M}$ . Using the absolute ground state space  $\mathcal{M}_q$  leads to a different definition of vortex cores of field-aligned vortices: the core is where Eq. (12) breaks down. This is why we call the region surrounding the tetrahedral vortices a “composite core.” The ordinary definition of a core arises when we focus on another space,  $\mathcal{S}$ , the sphere defined by  $|\psi| = \sqrt{n_0}$ . (This space minimizes the largest of the interaction terms,  $\frac{1}{2}\alpha n^2 - \mu n$ .) From the perspective of  $\mathcal{S}$ , a core would be a region where the wave function vanishes to avoid being discontinuous; however, in a spinor condensate with  $\alpha \gg \beta$ , the wave function never has to vanish because a closed loop cannot get snagged in the surface of the simply-connected sphere  $\mathcal{S}$ .

Now we have to classify both the topologies of the point vortices (or “tetrahedral charges”) and the composite vortices (or “aligned charges”), using the method described e.g. in [10]. For the point vortices we must parameterize the symmetry group that generates the composite core spin textures by a *simply connected* group  $G^*$ . We will take  $G^* = \{(g, \theta) | g \in SU_2 \text{ and } \theta \in \mathbb{R}\}$  where multiplication is defined by  $(g_1, \theta_1)(g_2, \theta_2) = (g_1 g_2, \theta_1 + \theta_2)$ . We parameterize  $G^*$  as follows,

$$D(e^{-i\alpha \frac{\hat{n}_\lambda \cdot \sigma}{2}}, \theta) = e^{i\theta - i\alpha \hat{n} \cdot \mathbf{F}}, \quad (13)$$

allowing us to regard  $G^*$  as a (redundant) description of the symmetries of the Hamiltonian. Using this representation, one can define the net vortex charge inside any closed loop  $\lambda$  (see Fig. 5a); one simply expresses the wave function along the loop in the form

$$\psi(\phi) = D(g(\phi), \theta(\phi)) \sqrt{n_0} \chi_3 \quad (14)$$

where  $\phi$  parameterizes the loop ( $0 < \phi < 2\pi$ ). In order for Eq. (14) to be continuous when the circuit is closed,  $\psi(\phi = 0) = \psi(\phi = 2\pi)$ , or

$$D(g(0), \theta(0)) \chi_3 = D(g(2\pi), \theta(2\pi)) \chi_3. \quad (15)$$

It follows that the “classifying group element” or net “topological charge” inside the curve

$$\Gamma(\lambda) = (e^{-i\alpha \lambda \frac{\hat{n}_\lambda \cdot \sigma}{2}}, \theta_\lambda) \equiv (g(0)^{-1} g(2\pi), \theta(2\pi) - \theta(0)) \quad (16)$$

is a symmetry describing the net rotation and rephasing around the closed loop. (Let us also use the briefer notation  $g_\lambda = e^{-i\alpha \lambda \frac{\hat{n}_\lambda \cdot \sigma}{2}}$  for the net rotation.) Since the tetrahedron has only 24 symmetries

(see Sec. IB), this makes for a tractable classification of the topologies. These topologies form the group of tetrahedral charges, multiplied together according to  $(g_1, \theta_1)(g_2, \theta_2) = (g_1 g_2, \theta_1 + \theta_2)$ .

When  $q$  is very large then Eq. (12) has to apply basically everywhere and when  $q$  is small then Eq. (12) has to apply outside of bound clusters of vortices. In order to classify the topology of vortices in the former case or of vortex clusters in the latter, we need a simply connected group that parameterizes the  $q \neq 0$  symmetry group  $e^{i\theta} e^{-i\alpha F_z}$ ; we take  $G_q^* = \{(\alpha, \theta) | \alpha, \theta \in \mathbb{R}\}$  and use the mapping  $D(\alpha, \theta) = e^{i\theta - i\alpha F_z}$ . Then we write  $\psi(\phi) = D_q(\alpha(\phi), \theta(\phi)) \sqrt{n_0} \chi_3$  and define

$$Q(\lambda) = (\alpha_\lambda, \theta_\lambda)_3 = (\alpha(2\pi) - \alpha(0), \theta(2\pi) - \theta(0))_3 \quad (17)$$

where the subscript 3 indicates that the magnetic field favors the 3-fold symmetric orientation illustrated in Fig. 2a (since we are assuming  $c > 4$ ), and the rotation through  $\alpha_\lambda$  is understood to be around the field axis. The possible values for  $Q$  can be referred to as “field-aligned charges” since they describe the topologies of vortex-fields in which the tetrahedra keep the orientation favored by the magnetic field.

Now let us consider the form of the fields near a tetrahedral vortex core. Near vortex  $i$ , the spin texture will be rotationally symmetric, and given by

$$\psi = e^{i\frac{\theta_i}{2\pi}\phi} e^{-i\frac{\alpha_i}{2\pi}\phi \hat{\mathbf{n}}'_i \cdot \mathbf{F}} \sqrt{n_0} \chi_0 \quad (18)$$

where  $\phi$  is now the azimuthal angle  $\phi$  centered at this vortex. Because the tetrahedra near this vortex may be tilted, we use  $\sqrt{n_0} \chi_0$ , a *generic* member of the cyclic order parameter space. The vortex is azimuthally symmetric since the parameters  $\theta_i, \alpha_i, \hat{\mathbf{n}}'_i$  are constants. The rotation axis  $\hat{\mathbf{n}}'_i$  is a local symmetry axis for the possibly *tilted* tetrahedra. To reduce the possible symmetries to a finite set, we should relate the spinor  $\chi_0$  to the spinor  $\chi_3$  corresponding to the tetrahedron as oriented in Fig. 2a. If we write  $\chi_0 = D(R, \xi) \chi_3$  for an appropriate rotation  $R$  and phase  $\xi$ , the vortex in Eq. (18) can be written

$$\psi(\phi) = D(R, \xi) e^{i\frac{\theta_i}{2\pi}\phi} e^{-i\frac{\alpha_i}{2\pi}\phi \hat{\mathbf{n}}_i \cdot \mathbf{F}} \chi_3, \quad (19)$$

where

$$\hat{\mathbf{n}}_i = R^{-1}(\hat{\mathbf{n}}'_i) \quad (20)$$

and we have used the transformation rule for angular momentum:

$$D(R, \xi)^\dagger F^i D(R, \xi) = \sum_{j=1}^3 R_{ij} F_j. \quad (21)$$

(The right-hand side uses the  $SO_3$  matrix  $R_{ij}$  associated with the rotation  $R$ .) Continuity implies that the rotation axis  $\hat{\mathbf{n}}_i$  is one of the finitely many symmetry axes illustrated in Fig. 2a; furthermore, according to the

above scheme, the group element that classifies this vortex is  $\Gamma_i = (e^{-i\alpha_i \frac{\sigma \cdot \hat{n}_i}{2}}, e^{i\theta_i})$ . There are only a discrete set of possible charges when we use  $\hat{n}_i$ , the axis relative to the body axes of the tetrahedron rather than  $\hat{n}'_i$ , the axis relative to the lab coordinates.

Eq. (19) expresses the vortex as a product of a constant matrix  $D(R, \xi)$  (the phase  $\xi$  is unimportant) and a standardized vortex configuration. The transformation  $D(R, \xi)$  rotates the standardized configuration in spin space, changing both the rotation axis (from  $\hat{n}_i$  to the local axis  $\hat{n}'_i$ ) and the orientation of the tetrahedra.

In the distant surroundings of a cluster of vortices, the spin texture will again have a rotationally symmetric form. The group element describing the change in the order parameter as one tours the loop  $\lambda$  enclosing the entire cluster is given by

$$\Gamma(\lambda) = \prod_i \Gamma_i. \quad (22)$$

This algebraic law has a few consequences. First, it leads to a conservation law that constrains vortex alchemy: the net charge  $\Gamma(\lambda)$  has to be conserved as the vortices inside the loop combine and metamorphose, since the topology on the loop cannot change suddenly. (There is only a discrete set of vortex charges because charges are defined using the body coordinates.) Second, Eq. (22) restricts the types of vortices which can form a cluster when  $q \neq 0$ . (See Fig. 5b.) Outside the cluster, the tetrahedra must be aligned with the field (see Eq. (12)), so the charge is described by a field-aligned order parameter  $Q(\lambda) = (\alpha, \theta)_3$ . Eq. (22) requires that

$$\prod_i g_i = e^{-i\alpha \frac{\sigma_z}{2}} \quad (23)$$

and  $\sum_i \theta_i \equiv \theta \pmod{2\pi}$ . The group elements must multiply to form a rotation about the  $z$ -axis to avoid the large Zeeman cost outside the clusters, or “composite cores” of the vortex molecules.

Let us now review the example in the previous section: the vortex molecule was made out of two vortices of type  $\Gamma_1 = (e^{-i\pi \frac{1}{2\sqrt{3}}(\sqrt{2}\sigma_x + \sigma_z)}, 0)$ ; since  $\Gamma_1^2 = (e^{-i\pi \frac{\sqrt{2}\sigma_x + \sigma_z}{\sqrt{3}}}, 0) = (-id, 0) = (e^{-i\pi\sigma_z}, 0)$ , the spin texture can align with the magnetic field outside the pair of vortices and  $Q = (2\pi, 0)_3$ . This uses the fact that, in  $SU_2$ , all  $2\pi$  rotations are equal to  $-id$ , where  $id$  is the  $2 \times 2$  identity matrix.

## B. Notation for Vortices with and without a Magnetic Field

Let us first assign names to the *tetrahedral* charges corresponding to closed loops in  $\mathcal{M}$ . At  $q = 0$  or within vortex clusters where  $q$  can be neglected, the topological charges are described by a pair  $\Gamma = (g, \theta)$  (defined in Eq. (16)) where  $g = e^{-i\alpha \frac{\hat{a} \cdot \sigma}{2}} \in SU_2$  and  $\theta \in \mathbb{R}$ . Note that

for the phase of the order parameter to be continuous, as Eq. (15) requires, the allowed values of  $\theta$  and  $g$  must be correlated [35, 37], so only a discrete sequence of phases may accompany a given rotational symmetry. Also note that in  $SU_2$ , rotation angles are defined modulo  $4\pi$  rather than  $2\pi$ . The twelve symmetries of the tetrahedron according to the ordinary method of counting become 24 because, e.g., a clockwise  $240^\circ$  rotation around an axis is distinguished from the counterclockwise  $120^\circ$  rotation. This is more than a technical point: the vortex where the order parameter rotates through  $-240^\circ$  about an order three axis cannot deform continuously into one where the order parameter rotates through  $120^\circ$ , and it has more energy as well. On the other hand, the  $\alpha = 4\pi$  “vortex” can relax continuously to a state free of vortices. The necessity of using  $SU_2$  instead of  $SO_3$  is the biggest surprise to come out of the topological theory.

Since  $g$  must be a symmetry of the tetrahedron corresponding to  $\sqrt{n_0}\chi_3$ , illustrated in Fig. 2a, we can describe  $g$  by indicating its rotation axis using the labels from the figure. We refer to the minimal rotation around a given axis using just the label of the axis; hence  $S, P, Q, R$  refer to the rotations through  $120^\circ$  counterclockwise as viewed from the tips of the corresponding arrows, and  $A, B, C$  refer to counterclockwise rotations through  $180^\circ$ , about  $A, B, C$ . Rotations through larger angles can be written as powers of these rotations. Therefore  $P^2$  is a  $240^\circ$  rotation; also  $P^3 = A^2 = -id$  since  $360^\circ$  rotations around any axis correspond to  $-id$  in  $SU_2$ . We find it convenient to describe each rotation as a rotation through an angle  $\alpha$  around some axis, where  $-2\pi \leq \alpha \leq 2\pi$ . (Positive and negative  $\alpha$ 's correspond to counterclockwise and clockwise rotations respectively.) An arbitrary rotation angle can be replaced by an angle in this interval using the fact that  $720^\circ$  rotations in  $SU(2)$  are equivalent to the identity. For example, the  $480^\circ$  counterclockwise rotation  $P^4$  is the same as the  $-240^\circ$  clockwise rotation  $P^{-2}$  because  $P^6$ , a rotation through two full turns, corresponds to the identity of  $SU(2)$ . On the other hand, the  $240^\circ$  counterclockwise rotation  $P^2$  is not equivalent to the clockwise  $120^\circ$  rotation around the same axis, since the corresponding  $SU(2)$  matrices differ by a minus sign.

Now we can list all the pairs of rotations and phases which are allowed by the continuity condition, Eq. (15). The possible vortices according to Ref. [35, 37] are  $(R^m, \frac{2\pi m}{3} + 2\pi n)$  and  $(A, 2\pi m)$  where  $n$  and  $m$  are integers, as well as the corresponding vortices with  $R$  replaced by  $P, Q$ , or  $S$  and  $A$  replaced by  $B$  or  $C$ .

One can work out explicit expressions for the  $SU(2)$  elements corresponding to given rotations. For example, let us find the  $SU(2)$  element corresponding to  $A$ ; since the rotation angle is  $180^\circ$ ,

$$A = e^{-i\pi \frac{\hat{a} \cdot \sigma}{2}} = -i\hat{a} \cdot \sigma, \quad (24)$$

where  $\hat{a}$  is the  $A$ -axis. Note that the tetrahedron has its vertices at  $(0, 0, -1), (-\frac{2\sqrt{2}}{3}, 0, \frac{1}{3}), (\frac{\sqrt{2}}{3}, \sqrt{\frac{2}{3}}, \frac{1}{3}),$



$(\frac{\sqrt{2}}{3}, -\sqrt{\frac{2}{3}}, \frac{1}{3})$ . The  $A$  axis bisects the segment connecting the last pair of points; the midpoint of these two points is

$$\frac{1}{2}(\hat{p} + \hat{q}) = (\frac{\sqrt{2}}{3}, 0, \frac{1}{3}). \quad (25)$$

The unit vector  $\hat{a}$  is obtained by normalizing this vector, so

$$\hat{a} = (\sqrt{\frac{2}{3}}, 0, \sqrt{\frac{1}{3}}). \quad (26)$$

Hence

$$A = -i\sqrt{\frac{2}{3}}\sigma_x - i\sqrt{\frac{1}{3}}\sigma_z. \quad (27)$$

The net charge, Eq. (22), of a set of vortices results from multiplying the matrices  $g$  for the vortices of the set. The result can be identified as one of the rotations  $A^n, B^n, P^n$ , etc. This procedure completely determines the  $SU(2)$  product element, whereas the geometric method of applying the appropriate sequence of rotations to a tetrahedron does not determine the *sign* of the  $SU(2)$  matrix.

We will describe a vortex reaction with the following notation,

$$(-id, 0) \rightarrow (R, \frac{2\pi}{3}) * (R, \frac{2\pi}{3}) * (R, -\frac{4\pi}{3}). \quad (28)$$

Each factor describes the charge of an individual vortex-atom, rather than a cluster of atoms, although  $(g, \theta)$  can be used to describe the net charge of a set of vortices as well, as in Fig. 5a. This reaction describes one point-vortex breaks up into three vortices. The  $*$  is just a separator between the different reaction products, reminding one to check conservation of charge by multiplying both sides of the reaction out.

Another useful cyclic spinor is

$$\chi_2 = \begin{pmatrix} \frac{1}{2} \\ 0 \\ -\frac{i}{\sqrt{2}} \\ 0 \\ \frac{1}{2} \end{pmatrix}. \quad (29)$$

This spinor corresponds to the tetrahedron in Fig. 2b. Its vertices are at the points of the form  $(\pm\frac{1}{\sqrt{3}}, \pm\frac{1}{\sqrt{3}}, \pm\frac{1}{\sqrt{3}})$  if we restrict the choices of signs so that there are always 0 or 2 minus signs. The fact that the  $A$ ,  $B$ , and  $C$  axes of this tetrahedron correspond to the  $\hat{x}$ ,  $\hat{y}$  and  $\hat{z}$  coordinate vectors makes the spinor  $\sqrt{n_0}\chi_2$  especially convenient for determining the consequences of the quadratic Zeeman term in the next section. The orientation of the tetrahedron in Fig. 2b is also very convenient for working out the group of charges, since the expressions for the symmetry axes

are so simple. (E.g.,  $\hat{p} = (\frac{1}{\sqrt{3}}, -\frac{1}{\sqrt{3}}, -\frac{1}{\sqrt{3}})$ , since vertex  $P$  is in the  $x > 0, y < 0, z < 0$  octant. Thus  $P = e^{-i\frac{2}{3}\hat{p}\cdot\sigma} = \frac{1-i\sigma_x+i\sigma_y+i\sigma_z}{2}$ .)

At nonzero magnetic field, only rotations around the  $z$ -axis are symmetries. When  $c > 4$ , the ground state space is  $\mathcal{M}_{q_3}$ , consisting of rotations and rephasings of  $\sqrt{n_0}\chi_3$ , as in Eq. (12). Vortices are described as in Eq. (17) by an ordered pair  $(\alpha, \theta)_3$  describing the rotation and rephasing angles of the vortex. The subscript 3 is used to indicate that the  $z$ -axis is an order three symmetry of the  $c > 4$  ground state tetrahedron. The continuity of the phase limits the vortex types to the form

$$Q = (\alpha, \theta)_3 = (\frac{2\pi m}{3}, 2\pi(\frac{m}{3} + n))_3. \quad (30)$$

When  $c < 4$ , minimizing Eq. (4) implies that the magnetic field axis is an order two symmetry, and the ground state space is  $\mathcal{M}_{q_2}$ , the rotations and rephasings of  $\sqrt{n_0}\chi_2$ . Now  $(\alpha, \theta)_2$  specifies the vortex types. The possibilities are

$$Q = (\alpha, \theta)_2 = (\pi m, 2\pi n)_2. \quad (31)$$

## II. ENERGIES AND SYMMETRIES

This section considers the effect of the magnetic field, which binds vortices, and the kinetic energy, which keeps the bound vortices from merging altogether. These are both included in the full energy function

$$\mathcal{H} = \iint d^2\mathbf{r} \frac{\hbar^2}{2m} \nabla\psi^\dagger \nabla\psi + V_{tot}(\psi), \quad (32)$$

where  $V_{tot}$  is given by Eq. (3). When  $B \neq 0$ , the Zeeman effect introduces an extra phase boundary dividing the cyclic phase into two phases, with a phase transition at  $c = 4$  where the tetrahedron changes its orientation relative to the magnetic field. (This result applies for moderate magnetic fields; very low magnetic fields cause different transitions[26].)

### A. The Anisotropy potential from the Quadratic Zeeman effect

Let us determine which orientations of the tetrahedron will be preferred by a magnetic field along the  $z$  axis. The preferred orientation can be calculated for small  $q$  from an effective potential which is a function of the orientation of the tetrahedron. As long as

$$q \ll n_0\beta, \quad (33)$$

the tetrahedron will be only slightly deformed. It will move into a space  $\mathcal{M}'$  displaced by a distance on the order of  $\frac{q}{n_0\beta}$  from the space  $\mathcal{M}$  of arbitrarily oriented

perfect tetrahedra. The spinors in the distorted space are given by

$$\psi = \sqrt{n_0}D(R, \xi)\chi_2 + \delta\psi, \quad (34)$$

where  $D(R, \xi)$  is the spin two rotation matrix corresponding to the rotation  $R$  of space, multiplied by a phase. The distortion  $\delta\psi$  depends on the orientation  $R$ . Eq. (11), which omits the deformation, is a harmless shorthand description, emphasizing the orientation of the tetrahedron. In this section, we use  $\sqrt{n_0}\chi_2$  as the standard spinor orientation instead of  $\sqrt{n_0}\chi_3$  to simplify calculating the energy; conveniently, the body axes  $A, B, C$  of the corresponding tetrahedron for the *former* state are aligned with the coordinate axes  $\hat{\mathbf{x}}, \hat{\mathbf{y}}, \hat{\mathbf{z}}$ . The body axes of the rotated state  $D(R)\sqrt{n_0}\chi_2$  (which make the angles  $\alpha_1, \alpha_2, \alpha_3$  with the  $z$ -axis) are thus  $R(\hat{\mathbf{x}}), R(\hat{\mathbf{y}}), R(\hat{\mathbf{z}})$ . Therefore the  $z$  component of the spin, in terms of the components of the spin along the body axes, is

$$D(R)^\dagger F_z D(R) = \cos \alpha_1 F_x + \cos \alpha_2 F_y + \cos \alpha_3 F_z. \quad (35)$$

At first order the quadratic Zeeman effect does not have any dependence on the orientation of the tetrahedron because a tetrahedral spinor is ‘‘pseudoisotropic,’’ i.e.,  $\chi_2^\dagger F_i F_j \chi_2 = 2\delta_{ij}$ . The first order energy is thus given by

$$\begin{aligned} \langle qF_z^2 \rangle &\approx n_0 q \chi_2^\dagger D(R)^\dagger F_z^2 D(R) \chi_2 \\ &\approx n_0 q \sum_{i,j=1}^3 \cos \alpha_i \cos \alpha_j \chi_2^\dagger F_i F_j \chi_2 \\ &\approx 2n_0 q, \end{aligned} \quad (36)$$

which does not prefer any orientation of the tetrahedron. In the last step we used

$$\sum_{i=1}^3 \cos^2 \alpha_i = 1 \quad (37)$$

which follows from the fact that  $\hat{\mathbf{z}}$ , a unit vector, has body-coordinates  $(\cos \alpha_1, \cos \alpha_2, \cos \alpha_3)$ .

To find the second order energy due to the quadratic Zeeman effect, which will break the tie, we have to find the deformed state and its energy. The deformation  $\delta\psi$  is determined by minimizing the total interaction and Zeeman energy in Eq. (3) for each given orientation  $R$ . Now if the deformation is not restricted somehow, the ‘‘deformation’’ which minimizes the energy will be very large, involving the tetrahedron rotating all the way to the absolute ground state. We therefore allow deformations only of the form

$$\begin{aligned} \delta\psi &= dD(R, \xi)\chi_2 \\ &+ \frac{1}{\sqrt{2}}(aD(R, \xi)F_x\chi_2 + bD(R, \xi)F_y\chi_2 + cD(R, \xi)F_z\chi_2) \\ &+ (e + if)D(R, \xi)\chi_{2t}, \end{aligned} \quad (38)$$

where  $a, b, c, d, e, f$  are real numbers. These terms correspond to the excitation modes found by [45]. This correction only perturbs  $\psi$  in 6 of the 10 directions in the Hilbert space. The other 4 directions are accounted for by the rotation  $R$  and the phase  $\xi$  which would be Goldstone modes when  $q = 0$ . (The energy remains  $\xi$ -independent even when  $q \neq 0$ .) The particular six stiff deformations in Eq. (38) are chosen because they are orthogonal to infinitesimal rotations and rephasings of the tetrahedral state. We have to find the deformations that minimize  $V_{tot}$ , Eq. (3), for each rotation  $R$ .

To evaluate  $V_{tot}$ , note that  $D(R, \xi)$  cancels from all the terms in the energy except for the Zeeman term, where one can use Eq. (35). The resulting expression for the energy density reads

$$\begin{aligned} V_{tot}(\psi) &= \frac{1}{2}\alpha(\tilde{\psi}^\dagger \tilde{\psi})^2 + \frac{1}{2}\beta(\tilde{\psi}^\dagger \mathbf{F}\tilde{\psi})^2 + \frac{1}{2}\gamma|\tilde{\psi}_t^\dagger \tilde{\psi}|^2 - \mu\tilde{\psi}^\dagger \tilde{\psi} \\ &- q \sum_{i,j=1}^3 \cos \alpha_i \cos \alpha_j \tilde{\psi}^\dagger F_i F_j \tilde{\psi} \end{aligned} \quad (39)$$

where  $\tilde{\psi} = \sqrt{n_0}\chi_2 + d\chi_2 + \frac{1}{\sqrt{2}}(aF_x\chi_2 + bF_y\chi_2 + cF_z\chi_2) + (e + if)\chi_{2t}$  is the perturbed wave function without the rotation. The effective potential Eq. (4) is obtained by minimizing  $V_{tot}$  over  $a, b, \dots$  while keeping  $R$  fixed. Further details are in Appendix A. (Working with  $\tilde{\psi}$  is equivalent to fixing the orientation of the tetrahedron and rotating the magnetic field.)

The effective potential suggests an analogue of the magnetic and charge healing length in condensates without magnetic fields (the ‘‘tetrahedron tipping length’’)—when the tetrahedra are rotated out of the appropriate ground state orientation at the edge of a condensate, the energy in Eq. (4) returns the order parameter to  $\mathcal{M}_q$  within the distance  $L_q \sim \frac{\hbar}{q} \sqrt{\frac{n_0 \beta}{m}}$ .

Now the ground states can be found as a function of  $c$ . When  $c > 4$ , a short calculation shows that Eq. (4) has its minimum at  $\cos \alpha_i = \pm \frac{1}{\sqrt{3}}$ ,  $i = 1, 2, 3$ ; i.e., when the magnetic field is along the line connecting a vertex of the tetrahedron to the opposite face or vertex. Hence the order parameter space  $\mathcal{M}_q$  is as given in Eq. (12). When  $c < 4$ , the effective potential is minimized by an orientation in which the field points parallel to the line joining a pair of opposite edges (see Fig. 2)[54].

The dependence of the ground-state orientation on  $c$  can be understood intuitively using the geometrical representation of Ref. [36]. In a tetrahedral state,  $\mathbf{m} = \psi^\dagger \mathbf{F}\psi = 0$  and  $\theta = \psi_t^\dagger \psi = 0$ , minimizing the interaction energies in Eq. (3). When a magnetic field is applied, the base of the tetrahedron illustrated in Fig. 2a gets pushed toward the vertex at  $-\hat{\mathbf{z}}$ . The tetrahedron in Fig. 2b, on the other hand, has its upper and lower edges pushed together, toward the  $xy$ -plane. Both these deformations move the spin roots (see [36]) away from the north and south poles, which increases the probability that  $F_z = \pm 2$  in the corresponding spinors, as favored by the quadratic Zeeman effect. Now these two types of

deformed tetrahedra have different spin-dependent energies. In the first case, the magnetization  $\mathbf{m}$  of the spinor becomes nonzero, increasing the  $\beta$  term of Eq. (3). In the second case, the magnetization of the spinor is still zero, by symmetry, but one can check that the spinor is no longer orthogonal to its time-reversal, so  $\theta$  is nonzero[55]. Therefore the orientation of the ground state tetrahedron is determined by whether the  $\mathbf{m}^2$  term or the  $|\theta|^2$  has a larger coefficient in the Hamiltonian. If the coefficient of the magnetization term is very large, then the state without any magnetization is preferred. The detailed calculation shows that the relevant comparison is between  $c\beta$  and  $4\beta$ .

The main source of anisotropy is different at sufficiently low magnetic fields[26]; the cubic Zeeman effect, proportional to  $B^3$ , then dominates over the effective potential in Eq. (4), proportional to  $B^4$ . Nevertheless the the order  $B^4$  effect we have calculated can dominate over the  $B^3$  effect, even when the magnetic field is small enough for the perturbation theory just described to apply. This is possible because the denominator  $n_0\beta$  in Eq. (4) is small compared to the hyperfine energy splitting  $A_{HF}$ . For spin 2 atoms the effect of the magnetic field is given by

$$V_{nz} = \psi^\dagger \sqrt{(\mu_B B)^2 + A_{HF}^2} \psi + A_{HF} \mu_B B F_z \psi \quad (40)$$

where  $A_{HF}$  is the hyperfine coupling. It follows that the quadratic and cubic Zeeman effects are  $qF_z^2 = \frac{\mu_B^2 B^2}{8A} F_z^2$  and  $\frac{\mu_B^3 B^3}{16A^2} F_z^3$ . The analysis we have given applies when the magnetic field is weak enough that the wave function is not drastically distorted, Eq. (33), but strong enough for the second order effect of the quadratic Zeeman term to dominate over the cubic Zeeman term. These conditions combine into

$$n_0\beta \ll \mu_B B \ll \sqrt{A_{HF} n_0\beta} \quad (41)$$

For  $^{87}\text{Rb}$  at density  $5 \times 10^{20}/m^3$ ,  $n_0\beta = 3$  nK and  $A_{HF} = 160$  mK while  $\mu_B = 67\mu\text{K}/\text{Gauss}$ ; hence the anisotropy potential used here is actually valid for a wide range of magnetic fields, between .04 mG and .3 G.

## B. Kinetic Energy

Now that we have estimated the energy due to misalignments with the quadratic Zeeman field, let us determine the kinetic energy of vortices in terms of the rotations and rephasings, Eq. (16). This energy will be the source of the repulsion that keeps the vortices apart within the vortex molecules. The kinetic energy is defined by the gradient terms in the Hamiltonian  $\mathcal{H}$ ; the analogue for liquid crystals is the elastic energy favoring alignment of the order parameter.

In order for the kinetic energy of a vortex to be minimal, the field on a circle around it should trace out a geodesic, as mentioned above. For the cyclic phase,

geodesics take the form given by Eq. (18). To see that vortices are geodesics as functions of  $\phi$ , suppose the field of a vortex is given far away by the radius independent expression

$$\psi(r, \phi) = \sqrt{n_0} F(\phi), \quad (42)$$

for an appropriate spinor function  $F(\phi)$ . The main contribution to the energy of this vortex is from the kinetic energy, which can be estimated by integrating from the core radius  $a_c \sim \hbar \sqrt{\frac{4\pi}{n_0\beta m}}$ . This is the same as the spin healing length (see [16] for the definition). The kinetic energy is

$$\begin{aligned} E &\approx \iint d^2\mathbf{r} \frac{\hbar^2}{2m} \nabla\psi^\dagger \cdot \nabla\psi \\ &\approx \int_0^{2\pi} n_0 |F'(\phi)|^2 d\phi \int_{a_c}^R \frac{\hbar^2}{2mr^2} r dr \\ &\approx \frac{\hbar^2 n_0}{2m} \ln \frac{R}{a_c} \int_0^{2\pi} |F'(\phi)|^2 d\phi \end{aligned} \quad (43)$$

Now the curve parameterized by  $F(\phi)$  adjusts itself so as to minimize the last integral, while maintaining the topology of the circuit traced out by  $F(\phi)$  in the order parameter space. One can show that an integral of this form is minimized when  $F(\phi)$  traces out a closed *geodesic* in the ground state space. The length of a closed curve is defined by  $\int_0^{2\pi} |F'(\phi)| d\phi$ , so it is not surprising that the geodesic of charge  $\Gamma$ , which minimizes this expression, also minimizes Eq. (43). Furthermore, if the geodesic has length  $l_\Gamma$ , then  $\int_0^{2\pi} d\phi |F'(\phi)|^2 = \frac{l_\Gamma^2}{2\pi}$ .

A geodesic in the cyclic order parameter space (which has the local geometry of a perfect sphere in four dimensions) can be described by a rotation at a fixed rate around a single axis as in Eq. (18). (For a shape less isotropic than a tetrahedron, the order parameter would rotate around a wobbling axis according to the rigid-rotation equations.) Substituting the symmetrical  $F(\phi)$  into Eq. (43) gives[44]

$$\begin{aligned} E &\approx \frac{\hbar^2 n_0}{2m} \ln \frac{R}{a_c} \int d\phi \psi^\dagger \left( -\alpha \frac{\hat{\mathbf{n}} \cdot \mathbf{F}}{2\pi} + \frac{\theta}{2\pi} \right)^2 \psi \\ &\approx \frac{\hbar^2 n_0}{4\pi m} \ln \frac{R}{a_c} \left[ \alpha^2 (n_i n_j Q_{ij} + \frac{s(s+1)}{3}) \right. \\ &\quad \left. - 2\alpha\theta n_i M_i + \theta^2 \right] \end{aligned} \quad (44)$$

where the general expression for any spin and phase has been given in terms of the quantum fluctuation matrix  $Q_{ij} = \frac{1}{n_0} (\psi^\dagger \frac{F_i F_j + F_j F_i}{2} \psi) - \frac{s(s+1)}{3} \delta_{ij}$  and the magnetization per particle  $M_i = \frac{m_i}{n_0}$ . The spin 2 tetrahedron state appears to be isotropic as long as one does not go beyond second order correlators, as seen from the following calculations:

$$\langle \chi_3 | F_i | \chi_3 \rangle = 0 \quad (45)$$

$$\langle \chi_3 | F_i F_j | \chi_3 \rangle = 2\delta_{ij} \quad (46)$$

and hence  $M = Q = 0$ . Eq. 44 implies that the energy is proportional to  $I_\Gamma^2 = (\theta^2 + 2\alpha^2)$ , a generalization of the Pythagorean theorem showing how to combine the amount of rephasing and rotation to get the total geodesic length. A spin rotation costs twice as much energy as a rephasing by the same angle.

In order to study vortex stability and Coulomb forces, let us define the “energy index,”

$$I_E = \left(\frac{l_\Gamma}{2\pi}\right)^2 = \left(\frac{\theta}{2\pi}\right)^2 + 2\left(\frac{\alpha}{2\pi}\right)^2, \quad (47)$$

which is a fraction for each tetrahedral charge from Sec. I B. The energy of a vortex is given as  $\frac{\pi\hbar^2 n_0}{m} \ln \frac{R}{a_c} I_E(\Gamma)$ , a multiple of the energy of an ordinary phase vortex. The force between a pair of vortices can be expressed very simply in terms of  $I_E$ .

The force follows from an estimate of the energy of a cluster of vortices. Using ideas from Ref. [46], we think of the cluster as forming the “core” of a bigger vortex, as illustrated in Fig. 6. (We are not necessarily assuming that the vortices are bound together.) Draw a circle of radius  $X$  just around the group of vortices. The kinetic energy can then be found as the sum of the energies outside and inside of  $X$ ; for the case illustrated in the figure this energy is approximately

$$\pi \frac{n_0 \hbar^2}{m} \left( [I_E(X) \ln \frac{R}{L_X}] + [(I_E(1) + I_E(2) + I_E(3)) \ln \frac{L_X}{a_c}] \right), \quad (48)$$

where  $L_X$  is the diameter of the group being combined together and  $R$  is the radius of whole system. The first term describes the energy outside of  $X$ . Sufficiently far outside of  $X$ , the field should have the form of a rotationally symmetric vortex. The rotation and rephasing of this vortex, measured along a circle outside  $X$ , is obtained by multiplying the group elements which describe all the individual vortices according to the rule for vortex unification Eq. (22). Hence the energy outside  $X$  is given by an expression like in Eq. (44), except that the integral must start at the radius  $L_X$  of the circle, so  $a_c$  must be replaced by  $L_X$ . The energy inside  $X$  is approximated by adding the energies of the three vortices in it, which are calculated like in Eq. (44) but now with  $R$  replaced by  $L_X$ .

This approximation makes a small error (compared to  $\ln \frac{L_X}{a_c}$ ) by ignoring the region where the vortices’ fields overlap. This error has a special scaling form if  $q = 0$  and if there are no other vortices in the condensate. In this case, the kinetic energy gives a complete description of the vortices outside their cores, and has a symmetry under rescaling. Therefore (as in [46]), one can show that the difference between Eq. (48) and the actual energy has the form

$$\Delta E = \frac{\pi n_0 \hbar^2}{m} f\left(\frac{L_{12}}{L_{13}}, \frac{L_{23}}{L_{13}}\right) + O\left(\frac{a_c}{L_X}\right) \quad (49)$$

where  $L_{ij}$  refer to the sidelengths of the triangle formed by the vortices. This correction can be ignored relative

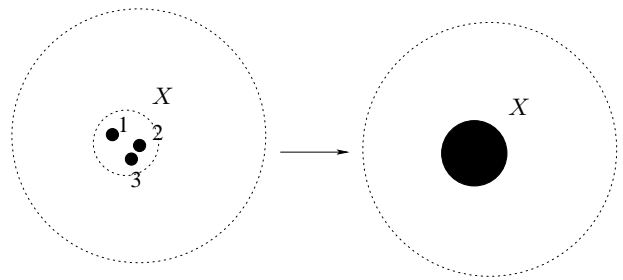


FIG. 6: A group of vortices is combined into the core of a composite vortex  $X$ . The energy outside the blacked-out “core” is calculated from the resultant winding number of the vortices inside, and the energy inside the “core” is calculated by looking inside the core to see which vortices are actually there.

to the logarithmically divergent terms kept in Eq. (48), as long as the side-lengths all have the same order of magnitude, since in this case  $f$  has no singularity.

The general expression for the energy of a set of vortices with charges  $\Gamma_i$ , after rearranging the formula to emphasize the dependence on the diameter of the set  $L$ , is:

$$E_K \approx \frac{\hbar^2 \pi n_0}{m} \left[ \sum_i I_E(\Gamma_i) - I_E\left(\prod_i \Gamma_i\right) \right] \ln \frac{L}{a_c} + \frac{\hbar^2 \pi n_0}{m} I_E\left(\prod_i \Gamma_i\right) \ln \frac{R}{a_c} \quad (50)$$

As long as the vortex cores are well-separated, the error in this estimate depends only on the ratios of the distances between the vortices, as in the three-vortex case, Eq. (49). The energy function has a similar form to the two-dimensional Coulomb interaction between vortices in an ordinary single-component condensate, and shows that the vortices repel or attract each other according as the index of the combined vortex is greater or less than the sum of the separate vortices’ indices. An interesting difference is that the interaction is *not* a sum of interactions of all pairs (consider three  $(A, 0)$  vortices, for example, or almost any other set of three vortices).

When there are just two vortices, the force between them can be calculated by differentiating Eq. (50), giving  $-\frac{\hbar^2 \pi n_0}{mL} [I_E(\Gamma_1) + I_E(\Gamma_2) - I_E(\Gamma_1 \Gamma_2)]$ . This is the *exact* (if  $L \gg a_c$  and  $q = 0$ ) expression for the force between the two vortices because the error (see Eq. (49)) reduces for two vortices to a constant. Improving on Eq. (50) depends on finding the spin texture in the overlap regions, and these equations are nonlinear when not all the vortices use the same symmetry axes.

In the next section, we will apply Eq. (50) more broadly. When there is a small cluster of vortices of size  $L$ , but there are some other vortices besides, the energy of just the vortices *in the cluster* can be estimated by replacing  $R$  in Eq. (50) by the distance  $D$  to the nearest vortex not in the cluster. Likewise, for  $q \neq 0$  the energy of a cluster with a net charge that is field-aligned can be

estimated by replacing  $R$  by  $L_q$ . As long as  $L \ll L_q$ , the detailed expression for the energy has the form given by Eq. (49), but when  $L$  approaches  $L_q$ , the anisotropy energy starts to compete with the kinetic energy and to distort the spin texture around the vortices.

### III. CHEMISTRY OF VORTICES

In this section we will first discuss stability of isolated tetrahedral vortices and then determine when these vortices can combine to form molecules (and what the spin texture around a molecule looks like). Some of these molecules are only metastable and can each break up in several ways.

Bound states of vortices will be formed out of stable tetrahedral vortices. These are the vortices based on  $120^\circ$  symmetries of a tetrahedron, accompanied by a phase shift of  $\frac{2\pi}{3}$  or  $-\frac{4\pi}{3}$ , and vortices based on  $180^\circ$  symmetries without a phase shift. Vortices with larger rotations or phase shifts will not occur as components of molecules. The net charge of the bound state must be field-aligned, with a schematic relation

$$Q = \prod_i \Gamma_i \quad (51)$$

between the field-aligned charge and the component charges. A composite vortex is stable if Coulomb repulsions can prevent the collapse of any subset of its components; since the Coulomb interaction is not a sum of pairwise interactions, it is not enough that every pair of vortices repel each other. Finally any bound state whose charge  $Q = (\alpha, \theta)_3$  has big enough rotation or rephasing angles can in principle decay into molecules with less energy, but this can only occur if thermal energy overcomes the Coulomb repulsion between the component vortices. The following expands on this general picture and points out some interesting sidelights.

#### A. Stable Tetrahedral Vortices

Only stable vortices will be found in the core-region of composite vortices. Since a weak anisotropy term can be neglected near component vortices, we can enumerate the stable vortex types assuming that  $q = 0$ .

Absolute stability of a vortex with charge  $\Gamma$  implies that if  $\Gamma$  is forced to break up into the fragments  $\Gamma_i$ , then the energy of the fragments grows as they separate from one another. The energy of the fragments can be found by applying Eq. (50). Note that  $\prod_i \Gamma_i = \Gamma$  by conservation of charge. If  $\Gamma$  has phase and rotation angles  $\theta$  and  $\alpha$  then

$$E_{\text{fragments}} \approx \frac{n_0 \hbar^2}{4\pi m} \left[ \sum_i (\theta_i^2 + 2\alpha_i^2) - (\theta^2 + 2\alpha^2) \right] \ln \frac{L}{a} + \text{const.} \quad (52)$$

Thus, if  $\sum_i (\theta_i^2 + 2\alpha_i^2) < (\theta^2 + 2\alpha^2)$ , the energy decreases as the vortices move apart, so the fragments will move apart by themselves the rest of the way. On the other hand, the vortex is absolutely stable if

$$\sum_i \left( \frac{\theta_i}{2\pi} \right)^2 + 2 \left( \frac{\alpha_i}{2\pi} \right)^2 > \left( \frac{\theta}{2\pi} \right)^2 + 2 \frac{\alpha^2}{2\pi}$$

for every set of  $\Gamma_i = (e^{-i\frac{\alpha_i \sigma \cdot \hat{n}_i}{2}}, e^{i\theta_i})$  such that  $\prod_i \Gamma_i = \Gamma$  (53)

Any tetrahedral vortex not satisfying this ‘‘absolute stability criterion’’ can break up into a lower-energy state, and we will assume that this break-up happens spontaneously for these *component* vortices. For example, the vortex  $(id, 4\pi)$  should break up into two  $(id, 2\pi)$ ’s, halving the energy. (In fact, these two singly quantized vortex can break up even further.) Generalizing this example, any vortex with charge  $(g, \theta)$  whose circulation  $\theta$  is bigger than  $2\pi$  can break up into  $(g, \theta - 2\pi)$  and  $(0, 2\pi)$  since  $\theta^2 > (2\pi)^2 + (\theta - 2\pi)^2$ . This leaves only finitely many vortices that have the possibility of being stable: all the ones with phase winding numbers not more than  $2\pi$ . Some of the vortices with  $|\theta| \leq 2\pi$  are also unstable; trial and error finds decay processes such as:

1.  $(-id, 0) \rightarrow (C, 0) * (C, 0)$  or  $(R, 2\pi/3) * (R, 2\pi/3) * (R, -4\pi/3)$ .
2.  $(-id, 2\pi) \rightarrow (R, \frac{2\pi}{3}) * (R, \frac{2\pi}{3}) * (R, \frac{2\pi}{3})$
3.  $(R^2, 4\pi/3)$  can break up into  $(R, 2\pi/3) * (R, 2\pi/3)$  and also  $(S^{-1}, 4\pi/3) * (C, 0)$
4.  $(R^2, -2\pi/3)$  might break up into  $(S^{-1}, -\frac{2\pi}{3}) * (C, 0)$ .
5.  $(C, 2\pi)$  could break up into  $(R, \frac{2\pi}{3}) * (S^{-1}, \frac{4\pi}{3})$ .

All of these decays lower the energy index. There are also two vortices which can break up without the energy indices changing:

1.  $(0, 2\pi)$  has the same charge as  $(R, \frac{2\pi}{3}) * (R^{-1}, \frac{4\pi}{3})$ .
2.  $(R, -\frac{4\pi}{3})$  has the same charge as  $(P^{-1}, -\frac{2\pi}{3}) * (Q^{-1}, -\frac{2\pi}{3})$ .

The energy may either increase or decrease after one of these processes, the logarithmic term which dominates the energy (see Eq. (50)) does not change, so the remainder term needs to be calculated to determine whether these break-ups raise or lower the energy. A point vortex whose charge is  $(0, 2\pi)$  is probably unstable if  $\alpha \gg \beta$  because a pure phase vortex has to have an empty core (with energy density of order  $\alpha n_0^2$ ), while the two fragments it breaks up into just have non-cyclic cores (energy of order  $\beta n_0^2$ ). [56]

We can now enumerate the vortices which are stable, noting that some vortices (such as  $(P^2, \frac{4\pi}{3})$ ) can break up

similarly to the ones just listed on account of symmetry. The only vortex types that have not been eliminated are the vortex with one-third circulation,  $(R, 2\pi/3)$  (energy index  $\frac{1}{3}$ ) and the currentless vortex  $(C, 0)$  (energy index  $\frac{1}{2}$ ) as well as possibly  $(R, -\frac{4\pi}{3})$  (energy index  $\frac{2}{3}$ ), and also the inverses and conjugates of these.

### B. Vortex Molecules at $q \neq 0$ and their Spin Textures

In this section we will describe a qualitative wave function for the example in Section IA to illustrate how the field of a vortex molecule deforms in response to the anisotropy energy as one leaves the region containing the two vortices. We will then give the binding criteria which describe how to use group theory to check which sets of the stable tetrahedral vortices (from the previous section) can combine together to form a vortex molecule at a nonzero magnetic field.

A vortex with a charge that is not compatible with the magnetic field has an energy that grows proportionally to the area of the condensate. Eq. (23) shows that the vortices in a cluster can avoid this energy cost if they have a net charge corresponding to a rotation around the  $z$  axis. More specifically, a set of tetrahedral vortices, with topologies  $\Gamma_i$ , has to have a net topology of the form

$$\prod_i \Gamma_i = (R^m, \frac{2\pi m}{3} + 2\pi n). \quad (54)$$

The ‘‘molecule’’ can then have the rotational and phase windings  $(\alpha, \theta)_3 = (\frac{2\pi m}{3} + 4\pi j, 2\pi(\frac{m}{3} + n))_3$  at infinity, for any  $j$ . One example of a molecule for the  $\mathcal{M}_{q3}$  phase is the composite vortex discussed at the beginning,  $(A, 0)(A, 0)$ , which partner up to make a compound vortex with  $Q = (2\pi, 0)_3$  in the field-aligned condensate.

Writing a wave function that describes this example even qualitatively is a little more complicated than it sounded in Sec. IA. A possible wave function is illustrated in Fig. 7. We can build this wave function up in stages. The most obvious attempt at writing a wave function fails to eliminate the quadratic energy cost:

$$\psi_{misalign} = e^{-\frac{i}{2}(\phi_1 + \phi_2)(\sqrt{\frac{2}{3}}F_x + \frac{1}{\sqrt{3}}F_z)} \sqrt{n_0} \chi_3, \quad (55)$$

where  $\phi_i = \arctan \frac{y-y_i}{x-x_i}$  is the polar angle measured with respect to the location  $(x_i, y_i) = \pm(\frac{L}{2}, 0)$  of the  $i^{\text{th}}$  vortex. The two  $180^\circ$  rotations about  $A$  combine into a  $2\pi$  rotation on a circle surrounding both vortices, but not about the magnetic field axis. *This* wave function takes the form  $\psi \approx e^{-i\phi \frac{1}{\sqrt{3}}(\sqrt{2}F_x + F_z)} \sqrt{n_0} \chi_3$  at infinity where  $\phi_1$  and  $\phi_2$  approach  $\phi$ . The tetrahedra rotate around a tilted axis, so they do not stay aligned appropriately with the magnetic field except on the  $x$ -axis and the  $y$ -axis (where the tetrahedra are reversed, but this is still a ground-state). The Zeeman energy of  $\psi_{misalign}$  is still infinite. This wave function agrees pretty well with the

one illustrated in the figure *within* the region surrounded by the large circle. The vortex cores are cordoned off by the small circles, where the  $180^\circ$  symmetry axes are marked by dots. Note that the tetrahedra three rows inside the large circle behave like the tetrahedra at infinity described by Eq. (55); they rotate through  $360^\circ$  about the order-two axis bisecting their right edge, producing all sorts of arbitrary orientations.

Another attempt, which uses the  $R$  axis instead of the  $A$  axis to eliminate the tilting of the tetrahedra,

$$\psi_{discontinuous} = e^{-\frac{i}{2}(\phi_1 + \phi_2)F_z} \sqrt{n_0} \chi_3, \quad (56)$$

is a complete fiasco, since this function is not continuous along the line connecting the two cores. (The  $R$  axis has the wrong symmetry, so as  $(x, y)$  circles around  $(x_2, y_2)$ ,  $\psi_{discontinuous}$  changes from  $\chi_3$  to  $e^{-i\pi F_z} \chi_3 \neq \chi_3$ .)

Luckily, since a  $2\pi$  rotation around one axis can be deformed to any other ( $2\pi$  rotations all correspond to  $-id \in SU_2$ ) one can produce a spin texture which has a finite Zeeman energy and is continuous. A hybrid of Eqs. (55) and (56) which achieves this, illustrated in Fig. 7, is:

$$\begin{aligned} \psi = & e^{-i\phi(F_x \sin \mu(r) + F_z \cos \mu(r))} e^{i\phi \frac{\sqrt{2}F_x + F_z}{\sqrt{3}}} \\ & \times e^{-\frac{i}{2}(\phi_1 + \phi_2)(\sqrt{\frac{2}{3}}F_x + \frac{1}{\sqrt{3}}F_z)} \sqrt{n_0} \chi_3 \end{aligned} \quad (57)$$

where  $\mu(r)$  must satisfy

$$\mu(0) = \arccos \sqrt{\frac{1}{3}} \quad (58)$$

$$\mu(\infty) = 0 \quad (59)$$

For example, we could define

$$\cos \mu(r) = \sqrt{\frac{r^2 + D^2}{r^2 + 3D^2}} \quad (60)$$

where  $D$  is a variational parameter. (Probably  $D \sim L$  is optimal.)

This field has two vortices at  $(\pm \frac{D}{2}, 0)$ . The texture varies continuously, except at the very centers of the vortices. (In the figure, the cores are inside the small circles. The tetrahedra’s orientations change rapidly around the circles’ centers, but each tetrahedron inside has a similar orientation to the tetrahedron next to it outside the circle.) Around the cores, the tetrahedra rotate around a tilted  $\hat{n}'$  axis which is aligned with the symmetry axis of the tilted tetrahedra around the vortex; the tilting is carried out by the rotations described by the first two factors in Eq. (57), just as discussed in Section IA. Near vortex 1, the wave function is approximately

$$\psi \approx e^{-\frac{i\phi_1}{2}(\sqrt{\frac{2}{3}}F_x + \sqrt{\frac{1}{3}}F_z)} \sqrt{n_0} \chi_3 \quad (61)$$

and near vortex 2,

$$\begin{aligned} \psi \approx & e^{-i\pi(F_x \sin \mu(\frac{L}{2}) + F_z \cos \mu(\frac{L}{2}))} \\ & e^{-\frac{i\phi_2 + i\pi}{2}(\sqrt{\frac{2}{3}}F_x + \sqrt{\frac{1}{3}}F_z)} \sqrt{n_0} \chi_3. \end{aligned} \quad (62)$$

(The local symmetry axis  $\hat{n}'$  is the rotation of the standard axis  $\sqrt{\frac{2}{3}}\hat{x} + \sqrt{\frac{1}{3}}\hat{y}$ , through a half-turn about  $\hat{x} \sin \mu(\frac{L}{2}) + \hat{y} \cos \mu(\frac{L}{2})$ , according to Eq. (18).)

Though the two tetrahedra are rotated into misaligned positions inside the large circle, the excursions from  $\mathcal{M}_{q3}$  to  $\mathcal{M}$  are brief and therefore cost only a finite amount of energy. Indeed, the first two factors fix the field up at infinity by applying a continuously varying rotation to the overall texture. These factors change the axis from  $A$  to  $R$  at large  $r$  as one can see by replacing  $\phi_1 \approx \phi_2$  by  $\phi$  and using Eq. (59):

$$\psi \rightarrow e^{-i\phi F_z} \sqrt{n_0} \chi_3. \quad (63)$$

The  $360^\circ$  axis changes from the  $A$  axis to the  $R$  axis as one crosses through the transition region indicated by the large circle in Fig. 7. As you follow a radius outward past the circle, the tetrahedra are tipped by different amounts. (The tetrahedra on the negative  $x$ -axis have to be tipped the most, though their original orientation is compatible with the magnetic field! The face which is on top is changed. This reorientation is required to make the amount of tipping continuous: the tipping angle increases more and more as  $\phi$  goes from 0 to  $\pi$ .)

The first two factors manage to fix the orientation at infinity without introducing discontinuities like in Eq. (56). Although they seem to have a vortex-like discontinuity at the origin, their discontinuous parts cancel on account of Eq. (58). (Hence the tetrahedra near the origin in Fig. 7 all have roughly the same orientation.) In short, though  $(A, 0)^2 = (-id, 0)$ , the cancellation of the Zeeman energy at infinity is not automatic! The topological classification just implies that the field in Eq. (55) *can* be deformed as  $r \rightarrow \infty$  so that the Zeeman energy is small.

The kinetic energy of this composite vortex, according to Eq. (50), is

$$E_K \approx \frac{\hbar^2 \pi n_0}{m} [2I_E((A, 0)) - I_E((-id, 0))] \ln \frac{L}{a_c} + \frac{\pi \hbar^2 n_0}{m} I_E((-id, 0)) \ln \frac{R}{a_c}. \quad (64)$$

Since  $I_E((A, 0)) = \frac{1}{2}$  and  $I_E(-id, 0) = 2$ , the coefficient of the first term is negative, so the vortices are driven apart in order to decrease the kinetic energy. This effect competes with the anisotropy energy, which tries to bring the vortices together. The net energy is therefore

$$E \approx f(D/L) \frac{q^2 D^2}{\beta} + \pi \frac{n_0 \hbar^2}{m} (2 \ln \frac{R}{L} + \ln \frac{L}{a}). \quad (65)$$

This is a more complete version of Eq. (8).  $f$  summarizes the dependence of the anisotropy energy Eq. (4) on  $D$  and  $L$ , but is too complicated for us to figure out!

The competition between the attractive Zeeman-term and the repulsive kinetic-energy term determines the size

of the vortex. Assuming  $D = L$  and minimizing over  $L$  gives

$$L \sim L_q = \frac{\sqrt{\frac{n_0 \hbar^2 \beta}{m}}}{q}. \quad (66)$$

This composite core-size is also the scale for the decay of tipping of tetrahedra due to the competition of anisotropy and kinetic energy (see Sec. II A), just as the core size of a spin vortex in a spin 1 condensate is equal to the magnetic healing length. Vortex molecules will have a size of the same order of magnitude (even if there are more than 2 subvortices) except when the component vortices have a short-range repulsion, like the two examples at the end of Section III A. (Such components form smaller molecules; vortices never form larger molecules. If a pair of tetrahedral vortices is stretched beyond  $L_q$ , a ‘‘cord’’ of tipped-tetrahedra forms between them, a simple version of the string imagined to hold the quarks together in a rapidly-rotating baryon.)

To find the total energy of the molecule, substitute  $L$  into Eq. (65) and simplify using  $a_c = \hbar \sqrt{\frac{4\pi}{n_0 \beta m}}$ :

$$E_{vortex} \sim 2\pi \frac{n_0 \hbar^2}{m} \ln R \frac{\sqrt{mq}}{\hbar} \quad (67)$$

We have dropped the contribution from the quadratic Zeeman term since it adds something that is independent of  $q$ .

This formula can be compared to the energy one expects for a *simple* vortex with the same charge  $(2\pi, 0)_3$ :

$$E_{vortex} = I_E((2\pi, 0)_3) \pi \frac{n_0 \hbar^2}{m} \ln \frac{R}{a'_c} + \epsilon_c \quad (68)$$

which includes a core energy  $\epsilon_c$  and allows for a physical definition of the core size. If we take  $a'_c$  to be the size of the molecule,  $L_q = \frac{1}{q} \sqrt{\frac{n_0 \hbar^2 \beta}{m}}$ , then the core energy has to be

$$\epsilon_c \approx \pi \frac{n_0 \hbar^2}{m} \ln \frac{n_0 \beta}{q}. \quad (69)$$

The core energy becomes large as  $q \rightarrow 0$  because the kinetic energy of the component vortices diverges as the logarithm of the core size  $L_q$ .

It makes sense to regard this composite vortex as a molecule because Coulomb repulsion keeps the vortices in the core separate. The previous discussion can be generalized by listing a set of binding criteria; these ensure that a set of tetrahedral vortices will form a stable or metastable composite vortex:

1. Each component vortex is one of the stable  $q = 0$  vortices from Section III A.
2. The kinetic energy is not decreased when any subset of the component vortices coalesces into a single vortex.

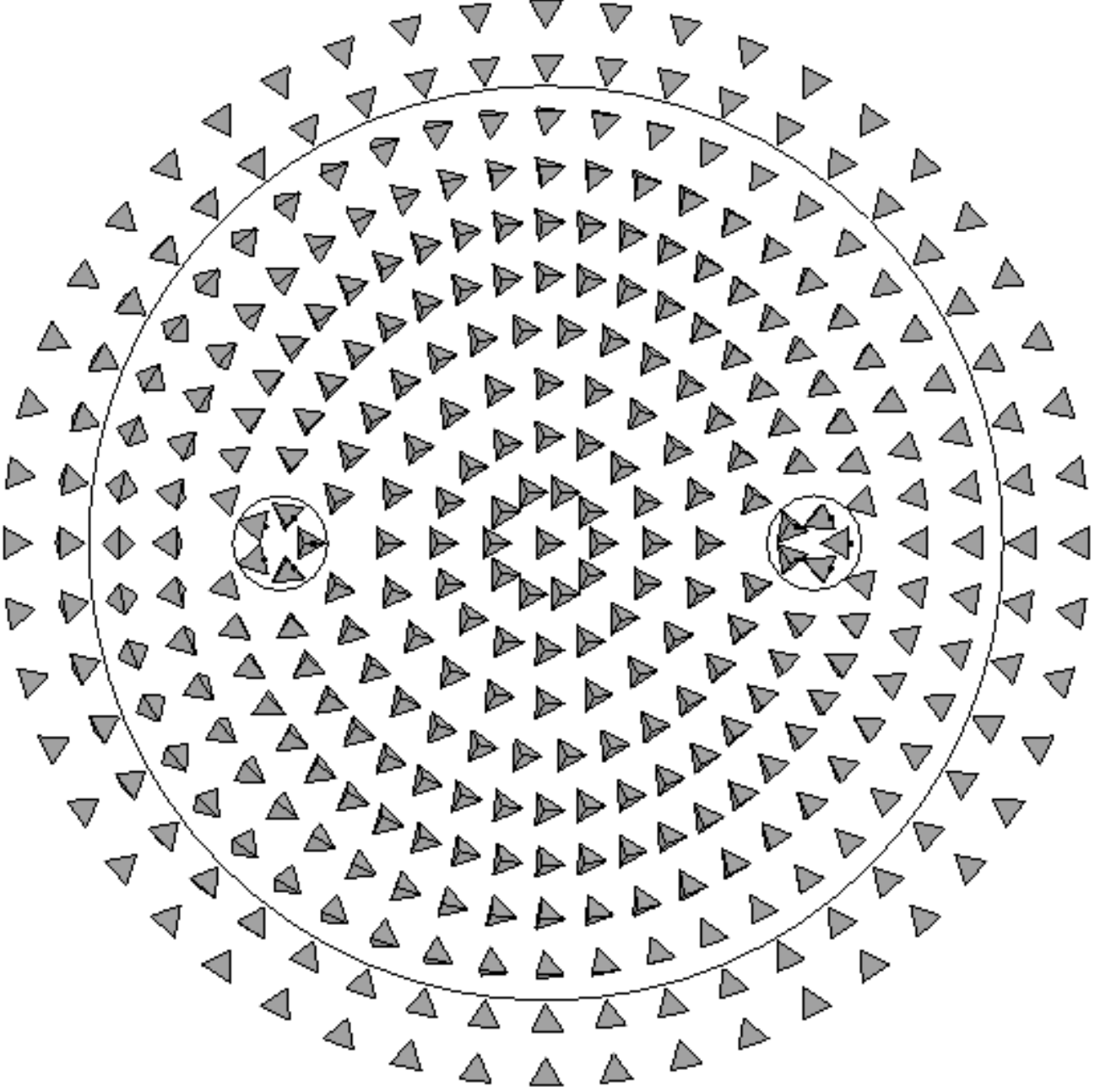


FIG. 7: An illustration of the composite vortex  $(A, 0) * (A, 0)$ . The magnetic field is perpendicular to the figure, so the tetrahedra prefer to be oriented with a face or a vertex facing up (since  $c > 4$ ). The two small circles enclose the  $180^\circ$  vortices, with symmetry axes indicated by black dots. The large circle indicates the transition region where the axis of the  $360^\circ$  rotation changes relative to the tetrahedra, from the  $A$  to the  $R$  axis. The figure uses a functional form with a rapid jump for  $\mu(r)$  (unlike in Eq. (60)) for simplicity, so that the transition region does not overlap the cores. For the probably more realistic form given by Eq. (60), the tetrahedra are already tipped at the centers of the vortices so that the local rotation axes  $\hat{n}'_i$  do not have the standard orientations illustrated in Fig. 2a.

3. There is no way for the component vortices to form submolecules that can break apart. This would occur if the components could be rearranged and then partitioned into  $r$  sets

$$\{\Gamma_1, \Gamma_2, \dots, \Gamma_{j_1}\}, \{\Gamma_{j_1+1}, \Gamma_{j_1+2}, \dots, \Gamma_{j_1+j_2}\}, \dots, \\ \{\Gamma_{j_1+j_2+\dots+j_{r-1}+1}, \Gamma_{j_1+j_2+\dots+j_{r-1}+2}, \dots, \Gamma_{j_1+j_2+\dots+j_r}\} \\ \text{such that each subset forms a molecule that is compatible with the magnetic field (i.e.,}$$



$\prod_{i=j_1+\dots+j_{k-1}+1}^{j_1+\dots+j_k} \Gamma_i = (R_k^m, 2\pi(\frac{m_k}{3} + n_k))$  and such that the sum of the energy indices of these submolecules is less than the energy index of the original molecule.

The vortex molecule  $(A, 0) * (A, 0)$  clearly satisfies all these conditions: Condition 1 is satisfied because  $(A, 0)$  is one of the stable vortices found in Section III A. Condition 2 is satisfied because the vortices repel each other. Condition 3 is easy to check for a diatomic molecule like this one, since it can only break up into individual “atoms”; neither of the fragments  $(A, 0)$  is compatible with the magnetic field.

### C. Metastable Vortices and How They Decay

Not all of the vortex molecules satisfying the three conditions above are *absolutely* stable. The analogue of the absolute stability condition, Eq. (53), also selects a finite set of *aligned* vortex types when  $q \neq 0$ , this time from among the group elements listed in Eq. (30). The absolutely stable charges are

$$\pm(\frac{2\pi}{3}, \frac{2\pi}{3})_3, \pm(\frac{2\pi}{3}, -\frac{4\pi}{3})_3. \quad (70)$$

For any *other* vortex topology  $Q = (\alpha, \theta)_3$ , one can find vortex topologies  $Q_i$  such that  $\prod_i Q_i = Q$  and

$$I_E(Q) > \sum_i I_E(Q_i). \quad (71)$$

*Point* vortices with such a topology  $Q$  would likely break apart spontaneously.

There is actually another pair of charges that could be absolutely stable, but the energy index estimate is not accurate enough to decide the issue:

$$(0, \pm 2\pi)_3, (\pm \frac{4\pi}{3}, \mp \frac{2\pi}{3})_3 \quad (72)$$

These vortices can break up into pairs without changing the net energy indices, reprising the ambiguous behavior of the two vortices at the end of Sec. III A. (See Section IV B for an answer.)

There are some *composite* vortices of other charges besides the four listed in Eq. (70) which are long-lived. The absolute stability criterion misses this possibility because it ignores the details of the vortex cores, drawing all its conclusions from the topology of the vortices far away: Suppose the initial vortex  $Q$  is a cluster of vortices with topologies  $\Gamma_1, \Gamma_2, \dots, \Gamma_r$  (see Fig. 8). The decay products discussed in the previous paragraph,  $Q_i$ , may be the combined topology of other vortex clusters. The energy of the vortices after the reaction (Fig. 8b) is smaller if

$$\begin{aligned} E_{init} &= I_E(Q)\pi\frac{n_0\hbar^2}{m}\ln\frac{R}{L} + k\ln\frac{L}{a_c} \\ &> \sum_i [I_E(Q_i)\pi\frac{n_0\hbar^2}{m}\ln\frac{R}{L} + k_i\ln\frac{L}{a_c}] = E_{fin}; \quad (73) \end{aligned}$$

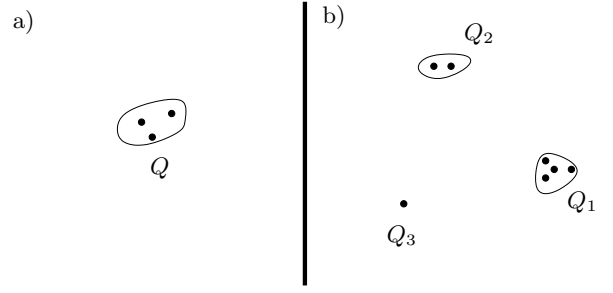


FIG. 8: Illustration of the absolute stability criterion. A composite vortex (a) and a possible set of composite vortices (b) it can break up into. Even if  $Q = Q_1Q_2Q_3$  and  $I_E(Q) > I_E(Q_1) + I_E(Q_2) + I_E(Q_3)$  so that the energy would decrease, the break-up might not occur spontaneously. If the component vortices in (b) are different from the component vortices in (a), then the vortices making up  $Q_1$ ,  $Q_2$ , and  $Q_3$  would have to be produced in a “chemical” reaction from the components of  $Q$ .

The terms proportional to  $\ln\frac{R}{L}$  stand for the kinetic energies outside the composite cores, and the terms proportional to  $\ln\frac{L}{a_c}$  stand for the energies within the composite cores; the latter contributions do not matter once the composite vortices are far apart ( $R \gg L$ ). Therefore, the energy-index relation, Eq. (71), implies that the energy decreases when  $Q \rightarrow Q_1 * Q_2 * \dots * Q_r$ .

However, at zero temperature, a vortex molecule satisfying the binding criteria *cannot* break up, even if the total energy would end up smaller. Although the metamorphosis of Fig. 8a into Fig. 8b lowers the energy, the process will not occur spontaneously. According to condition 3, the vortices in Fig. 8b are different than those in Fig. 8a. And according to conditions 1 and 2, there are no spontaneous chemical reactions that can occur to make the components in Fig. 8b out of those in Fig. 8a. Thus, at zero temperature, composite vortices besides the ones with charges listed in Eq. (70), whose energy indices seem to be too big, can still be stable. At *nonzero* temperature, such a molecule will only be metastable because it can decay after reactions inside its core produce the vortex types that appear in Fig. 8b. These reactions are prevented by energy barriers, so the decay will occur only after a long time.

The vortex molecule made up of  $(A, 0) * (A, 0)$  is an example of a metastable vortex; its charge  $(2\pi, 0)_3$  did not appear in Eq. (70) because it is the same as the net charge of the three *field-aligned* point vortices  $(\frac{2\pi}{3}, \frac{2\pi}{3})_3 * (\frac{2\pi}{3}, -\frac{4\pi}{3})_3 * (\frac{2\pi}{3}, \frac{2\pi}{3})_3$ . The energy index of the molecule is  $2(1^2) + 0^2$  (see Eq. (47)) while the energy index of the three point vortices is smaller,  $\frac{1}{3} + \frac{2}{3} + \frac{1}{3}$ . Nevertheless, since these three vortices are not present in the core of the original vortex the decay cannot occur spontaneously.

A vortex with a composite core can break up by a combination of vortex-fusion and vortex fragmentation. Some subsets of the original component vortices fuse and the fused vortices each break up into some other vortices.

These regroup into clusters each of which has a charge compatible with the magnetic field. Then each cluster goes its own way. (The fusion and fragmentation steps might sometimes happen more than once.) Conditions 1 and 2 ensure that at least one of these steps will be opposed by the Coulomb potential, but the *total* energy will decrease if the energy index decreases. The vortex molecule will be long-lived because its components do not know that the hard effort of fusing will allow them to change into vortices which can separate.

Trial and error yields a couple of ways in which the  $(A, 0) * (A, 0)$  bound state can break up. One possibility begins with the two component vortices coalescing,

$$(A, 0) * (A, 0) \rightarrow (-id, 0) \rightarrow (R, \frac{2\pi}{3}) * (R, \frac{2\pi}{3}) * (R, -\frac{4\pi}{3}) \quad (74)$$

The other begins when one of the components breaks up,

$$(A, 0) * (A, 0) \rightarrow [(R^{-1}, -\frac{2\pi}{3}) * (Q, \frac{2\pi}{3})] * (A, 0) \\ \rightarrow (R^{-1}, -\frac{2\pi}{3}) * [(Q, \frac{2\pi}{3}) * (A, 0)]. \quad (75)$$

In the first process, the two vortices come together, increasing the kinetic energy in accordance with Condition 2 (as shown by calculating the  $I_E$ 's and substituting into Eq. (50)). The resulting vortex breaks up into three vortices which can separate from each other because they are compatible with the magnetic field. The increase in energy during the first stage is given by  $E_{s1} - E_{init} = \pi \frac{n_0 \hbar^2}{m} \ln \frac{Lq}{a_c}$  where  $E_{s1} = \pi \frac{n_0 \hbar^2}{m} I_E(-id, 0) \ln \frac{R}{a_c}$  is the energy of the intermediate vortex. Thermal fluctuations have a chance of driving the  $(A, 0)$ 's together, in spite of the energy increase  $E_{s1} - E_{init}$ .

In the second process, Eq. (75), the  $(A, 0)$  vortex first splits up into two vortices. The first of these,  $(R^{-1}, -\frac{2\pi}{3})$  is compatible with the Zeeman field and can leave. The remaining two vortices form a new molecule which cannot break up because  $Q$  is a rotation around the wrong order 3 axis. For *this* process Condition 1 requires that the energy increases during the initial fragmentation. To check this, note that the energy of the intermediate state is

$$E_{s2} = \pi \frac{n_0 \hbar^2}{m} \{ [I_E(R^{-1}, -\frac{2\pi}{3}) + I_E(Q, \frac{2\pi}{3}) + I_E(A, 0)] \ln \frac{L}{a_c} \\ + I_E(-id, 0) \ln \frac{R}{L} \} \quad (76)$$

and the energy barrier is

$$E_{s2} - E_{init} \\ = \pi \frac{n_0 \hbar^2}{m} [(I_E(R^{-1}, -\frac{2\pi}{3}) + I_E(Q, \frac{2\pi}{3}) - I_E(A, 0)) \ln \frac{L}{a} \\ = \frac{\pi n_0 \hbar^2 m}{6} \ln \frac{L}{a}. \quad (77)$$

This energy barrier is lower than  $E_{s1} - E_{init}$ , so Eq. (75) is a more common break-up route. (In a finite condensate, thermally excited break-ups can be observed only

if a vortex molecule is somehow prevented from wandering to the boundary of the condensate and annihilating before it can decay.)

These two examples illustrate the meaning of the stability conditions. Conditions 1 and 2 ensure that fragmentation and fusion processes cannot happen spontaneously. The third condition simply points out that vortex clusters like  $(A, 0)^2 * (B, 0)^2$  will not be stable because the components can sort themselves into field-aligned groups and break up without any thermal assistance. The second condition can be difficult to check for a composite vortex with three or more sub-vortices. One must consider subsets of every size and check that they cannot lower their energy by collapsing all at once into one vortex. Just knowing that any two vortices of the subset *repel* each other does not guarantee that the set of vortices do not *collectively attract* each other! An example is the set of three vortices  $(A, 0)^3$ . Any two of these vortices would combine to form a vortex with a  $360^\circ$  rotation,  $(-id, 0)$ , whose index 2 is higher than the sum,  $\frac{1}{2} + \frac{1}{2}$ , of the indices of the collapsing pair. On the other hand all three vortices could form a vortex  $(A^{-1}, 0)$  with energy index  $\frac{1}{2} < 3I_E(A, 0)$ , so the three vortices can collapse simultaneously to lower the energy. An even more counterintuitive complication is that, because of the noncommutative behavior of the combination rules, more complicated fusion processes can occur. A vortex can change its type by circling around one vortex so that it can fuse with another vortex. (See Appendix B.) For a bound state of many vortices there will be many possibilities for how the vortices meander around each other before some of them fuse. To test Condition 3, one also has to enumerate all possible wanderings.

A mathematical statement of our results is that there will be (at least) one solution to the time-independent Gross-Pitaevskii equation for any set of vortex topologies that satisfy the three conditions. If  $q$  is small, the energy at the top of the barrier is greater, by a logarithmically large amount, than the energy of an initial variational state like the approximate wave function Eq. (57). A solution to the Gross-Pitaevskii equation should result if one starts from this qualitative texture and lets it relax to a local minimum of the energy. There is not enough energy for the wave function to get over the energy barrier, so the wave function should get stuck in a local minimum. (The energy of the intermediate state is not known precisely because of the rough estimates we have made of the Zeeman energy and the kinetic energy, but these errors are small compared to the height of the barrier.)

#### IV. ADDITIONAL EXAMPLES

Now we can construct some other, more interesting, examples. We will use the algebra of the group of vortex charges to find molecules whose net charge is interesting in different ways, and we will use the energy index to test

	Components	Net Charge	$c$	Stable?
1	$(A, 0) * (A, 0)$	$(2\pi, 0)_3$	$c > 4$	Metastable
2	$(P^{-1}, \frac{4\pi}{3}) * (Q^{-1}, \frac{4\pi}{3}) * (R^{-1}, \frac{4\pi}{3})$	$(0, 4\pi)_2$	$c < 4$	Metastable
3	$(Q, \frac{2\pi}{3}) * (A, 0)$	$(-\frac{4\pi}{3}, \frac{2\pi}{3})_3$	$c > 4$	Stable
4	None	$(4\pi, 0)_{2,3}$	Any value	Metastable

TABLE I: Examples of vortex molecules. The tetrahedral charges of the components of the molecules and the net aligned charge are given. The condition on  $c$  determines how the tetrahedra are oriented far from the vortex, due to the magnetic field. The final column indicates whether the vortex molecule is expected to have the absolute minimum energy of all vortices with a given net aligned charge. The second molecule might actually not be bound—see the text.

whether they are stable.

The parameter  $c$  will be less than 4 for some of these examples. If  $c < 4$  the ground state orientation of the tetrahedron will be as in Fig. 2b so the  $z$ -axis is an order 2 axis. The aligned topologies have the forms  $(\pi n, 2\pi m)_2$ , as described in Section IB. Of these, the only absolutely stable topologies are  $\pm(\pi, 0)_2$ ,  $\pm(0, 2\pi)_2$  (and possibly  $(\pm\pi, \pm 2\pi)_2$ ).

### A. A Doubly Quantized Pure Phase Vortex

First let us find a vortex molecule whose phase winds by  $4\pi$ . In single component condensates, such vortices are usually unstable; one has been observed to break up, maybe into an entwined pair of  $2\pi$  vortices[30]. If phase and spin textures were completely independent of one another, doubly quantized vortices would not be any more stable in the cyclic condensates; but fractional circulations are “bound” to certain spin textures (see Sec. IB). If we assume the vortex  $(R, -\frac{4\pi}{3})$  is stable (at the end of Sec. III A we could not decide), then a doubly-quantized vortex can occur in a cyclic condensate when  $c > 4$ . It consists of the three parts

$$(P^{-1}, \frac{4\pi}{3})(Q^{-1}, \frac{4\pi}{3})(R^{-1}, \frac{4\pi}{3}). \quad (78)$$

The phase changes by  $4\pi$  while the orientation of the tetrahedron does not change at infinity as we can check using the coordinate system from Fig. 2b. The three group elements are

$$\begin{aligned} P^{-1} &= \frac{1}{2}(1 + i(\sigma_x - \sigma_y - \sigma_z)) \\ Q^{-1} &= \frac{1}{2}(1 + i(\sigma_x + \sigma_y + \sigma_z)) \\ R^{-1} &= \frac{1}{2}(1 + i(\sigma_z - \sigma_x - \sigma_y)) \end{aligned}$$

and their product is the identity.

Let us discuss the conditions for binding. We have not checked Condition 1; it is not easy to check because  $(P^{-1}, \frac{4\pi}{3})$  has the same charge and energy index as  $(R, \frac{2\pi}{3}) * (Q, \frac{2\pi}{3})$ ; an accurate solution for the spin texture around this pair of vortices is needed. Besides,  $(P^{-1}, \frac{4\pi}{3})$  might be stable for some ranges of  $c$  values, but not others. Let us therefore hope that condition 1

is satisfied. Condition 3 is clear. To check condition 2, let us first consider whether one of the *pairs* of vortices in the trio can coalesce. Using conservation of topological charge helps to avoid enumerating all the ways the vortices can braid around each other. If the first two vortices have coalesced into a vortex  $(X, \frac{8\pi}{3})$  (after some permutation) and the third vortex, by winding around the other two vortices as they collapsed, has changed to  $(Y^{-1}, \frac{4\pi}{3})$ , then

$$(XY^{-1}, 4\pi) = (id, 4\pi) \quad (79)$$

by conservation of charge. Hence  $X = Y$ . Also, braiding one vortex between other vortices can only *conjugate* its group element. Therefore,  $Y$ , like  $R$ , is a counter-clockwise rotation through  $120^\circ$ . Since  $X = Y$ , the rotation part of the coalesced vortex  $(X, \frac{8\pi}{3})$  also is a  $120^\circ$  turn and thus the energy index of this coalesced vortex is  $2 \times (1/3)^2 + (4/3)^2 = 2$ , which is *greater* than the sum of the energy indices of the two vortices which formed it. Therefore the two vortices cannot coalesce spontaneously. (This argument can be generalized to any trio of vortices  $\Gamma_1, \Gamma_2, \Gamma_3$  each of which commutes with the net charge  $\Gamma$ . Fusing two of the vortices gives the same result (up to conjugacy) no matter how the vortices are mixed around first; so braiding cannot make a repulsive interaction between two vortices into an attractive one.) Finally, the three vortices cannot coalesce simultaneously because  $I_E(0, 4\pi) > I_E(P^{-1}, \frac{4\pi}{3}) + I_E(Q^{-1}, \frac{4\pi}{3}) + I_E(R^{-1}, \frac{4\pi}{3})$ .

### B. A Vortex Molecule which is Stable

Returning to the original assumption,  $c > 4$ , where the ground state orientation is illustrated by Fig. 2a, we can show that the second charge in Eq. (72) *does* correspond to a completely stable vortex molecule. In fact, consider

$$(Q, \frac{2\pi}{3})(A, 0). \quad (80)$$

This molecule, one of the decay products in Eq. (75), has the topology  $(R^{-2}, \frac{2\pi}{3})$  or (using the notation appropriate for the field-aligned tetrahedra outside the composite core),  $(-\frac{4\pi}{3}, \frac{2\pi}{3})_3$ . The energy of this molecule is approx-

imately

$$\begin{aligned} \frac{\pi n_0 \hbar^2}{m} [I_E(R^{-2}, \frac{2\pi}{3}) \ln \frac{R}{L_q} + I_E(Q, \frac{2\pi}{3}) \ln \frac{L_q}{a_c} + I_E(A, 0) \ln \frac{L_q}{a_c}] \psi(\phi; t) &= e^{-i\phi(F_x \sin \pi t + F_z \cos \pi t)} e^{-iF_z \phi} \sqrt{n_0} \chi_0, \quad (82) \\ &= \frac{n_0 \pi \hbar^2}{m} (\ln \frac{R}{a_c} - \frac{1}{6} \ln \frac{L_q}{a_c}). \quad (81) \end{aligned}$$

where  $L_q$  is the size of the composite core, given by Eq. (66).

This molecule answers a question from Section III C. Are there stable vortices with charge  $(-\frac{4\pi}{3}, \frac{2\pi}{3})_3$ ? The two vortices  $(-\frac{2\pi}{3}, -\frac{2\pi}{3})_3 * (-\frac{2\pi}{3}, \frac{4\pi}{3})_3$ , have the same net topology as a vortex of charge  $(-\frac{4\pi}{3}, \frac{2\pi}{3})_3$ , and they have the *same* net energy index. Now we can check that the composite vortex  $(Q, \frac{2\pi}{3})(A, 0)$  is a stable realization for the charge  $(-\frac{4\pi}{3}, \frac{2\pi}{3})_3$ . Its energy is lower *by a finite amount* than the energy  $\frac{\pi n_0 \pi \hbar^2}{m} (\frac{1}{3} + \frac{2}{3}) \ln \frac{R}{a_c}$  of the pair of vortices. This finite binding energy is  $\frac{\pi n_0 \hbar^2}{6m} \ln \frac{L_q}{a}$ .

To take another point of view, the minimum-energy spin texture with the topology  $(-\frac{4\pi}{3}, \frac{2\pi}{3})_3$  imposed far away has an asymmetric structure: it has two “singularities” with topologies  $(Q, \frac{2\pi}{3})$  and  $(A, 0)$  at a distance of order  $L_q$ . By contrast, when the topology imposed at a boundary corresponds to unstable vortices, the ground state has singularities whose spacing is on the order of the size of the system  $R$ . E.g., in a scalar one might try to impose  $\psi(R, \phi) = \sqrt{n_0} e^{2i\phi}$ . The spacing of the vortices in the energy minimizing wave function grows with  $R$ , reflecting the fact that these vortices would repel each other to infinity in an infinite condensate.

### C. A “Bound State” of No Vortices

The final example shows that point vortices are not necessary to hold a core together—there is a “composite” vortices without any components! In other words we can construct a vortex for which the order parameter stays in  $\mathcal{M}$ . There is still a “composite core” where the tetrahedra leave  $\mathcal{M}_q$  and are no longer aligned with the field axis. The trick is that the amount of rotation in a texture around a vortex is defined only modulo  $4\pi$ , in the absence of a magnetic field (because of the  $SU_2$  charge classification). When  $B$  is turned on, the spin part of the order parameter space  $\mathcal{M}_q$  has the same topology as a circle, so each additional winding by  $2\pi$  changes the topological charge. (A texture which rotates by  $4\pi$  about the field axis can relax only by using axes perpendicular to the magnetic field.) Thus a  $4\pi$ -rotation-vortex is stable in a magnetic field, but since it has zero *tetrahedral* charge, it does not have to have point vortices inside of it. (Another way to say this: Eq. (54) does not uniquely determine the aligned topology, because  $R^6 = id$ . Hence a  $(4\pi, 0)_3$ -vortex can be made from 6  $R$  vortices (i.e., some  $(R, \frac{2\pi}{3})$ 's and  $(R, -\frac{4\pi}{3})$ 's) or out of no vortices at all!)

Such vortices occur for both the  $c > 4$  and  $c < 4$  cases. A variational wave function can be constructed using the

formula that shows how a  $4\pi$  rotation-vortex can relax in the absence of a magnetic field:

where  $\chi_0$  is an arbitrary cyclic spinor. At each moment of time  $t$ , the expression describes an  $r$ -independent texture as a function of  $\phi$ . When  $t = 0$ , there is a vortex which is a full rotation through  $720^\circ$ . By the time  $t = 1$ , this vortex has completely dissipated. When  $q \neq 0$  a  $4\pi$  vortex cannot relax in this way because the tetrahedra rotate away from the orientation preferred by the magnetic field before returning to the preferred orientation at the end. But Eq. (82) has a reincarnation as the description of a  $(4\pi, 0)_{2,3}$  vortex. We replace the time coordinate by a function of the radius to give a spin texture that winds through  $4\pi$  at infinity but does not have any singularities at 0:

$$\psi = \psi(\phi; \frac{1}{1 + (\frac{r}{L})^2}). \quad (83)$$

If  $\chi_0 = \chi_2$  or  $\chi_3$ , then this wave function, at large  $r$ 's, has the winding number  $(4\pi, 0)_{2,3}$ . At small  $r$ 's, the wave function is  $\phi$ -independent, giving a continuous and “coreless” wave-function. (The exact solution not only has a more complicated  $r$ -dependence, but also a less-symmetrical  $\phi$ -dependence.) The region  $r \lesssim L$  is the composite core of this vortex in the sense that  $\psi \in \mathcal{M}$  rather than  $\mathcal{M}_q$ . The optimal size  $L$  of this region is again  $L_q$ , as balancing the kinetic and Zeeman energies shows.

This vortex cannot disappear because the classification of vortices at *nonzero*  $q$  implies that  $\alpha = 4\pi$  is conserved. Furthermore, though it does not satisfy the *absolute* stability criterion, since two  $(2\pi, 0)_{2,3}$ 's have a smaller energy, it is obviously metastable—there are no vortices in the core to break apart! The vortex can only break up if thermal energy causes a vortex-antivortex pair to nucleate in the core. Suppose a pair involving rotations through  $2\pi$  in *opposite* directions appears. These vortices initially attract each other but if the thermal fluctuations pull them to opposite sides of the core the nonlinear coupling with the background field switches this force from attractive to repulsive, and the vortices can separate the rest of the way by themselves.

## V. CREATING AND OBSERVING VORTEX MOLECULES

Let us discuss the conditions under which the Zeeman-effect bound states might be observed and the methods one can use for observing them. First of all, we must assume that  $q \ll \beta n_0$  in order to justify neglecting  $q$  near the tetrahedral vortices and to justify the perturbation theory of Sec. II A. This is not just a technical assumption: above a certain magnetic field the component vortices probably merge. To estimate the maximum

magnetic field note that  $q$  is related to the hyperfine splitting  $A_{HF}$  via

$$|q| = \frac{\mu_B^2 B^2}{8A_{HF}}, \quad (84)$$

for rubidium and sodium atoms[2], and similar relations hold for other atoms. Also note that the spin independent interaction is

$$\alpha = \frac{4\pi\hbar^2}{ma} \quad (85)$$

where  $a \sim 50 \text{ \AA}$  is an *average* of the scattering lengths corresponding to different net spins and that the spin dependent interaction is

$$\beta = \frac{4\pi\hbar^2\Delta a}{m} \quad (86)$$

where  $\Delta a \sim 1 \text{ \AA}$ [39, 41] depends on the *differences* between the scattering lengths[9]. The condition for our analysis to be applicable,  $q \ll n_0\beta$ , therefore implies

$$B \ll B_{Max} \sim \frac{1}{\mu_B} \sqrt{A_{HF} \frac{\hbar^2 n_0 \Delta a}{m}}, \quad (87)$$

about .1 G for a condensate of rubidium atoms with density  $n_0 = 5 \times 10^{14}/\text{cc}$ .

In order to observe vortex bound states, one might start with a condensate prepared with a spin order other than the ground state and then watch it evolve as in Ref. [16]. Thermal (and less importantly quantum) noise will produce perturbations that grow exponentially, producing complicated patterns. If the magnetic field is small enough, vortex bound states might be found after some time. To test whether these vortex bound states behave in the way we have been describing, one would have to identify the topological charges of the vortices. One could then check that vortex sets whose net charge is compatible with the magnetic field have a size on the order of the theoretical value,  $L_q$ . One may have to use statistical correlations if too many vortices stay around. (One could also take a more deliberate approach, choosing vortex types and imprinting them as in [47] or [28]. One can then observe the subsequent evolution of the vortices to see whether they bind together.)

In fact, identifying the vortices that appear in a spinor condensate is difficult; vortex cores in a spinor condensate are not empty like the vortices in an ordinary condensate; they have nearly the same density as the rest of the condensate[48]. One thus has to measure something about the spins to observe the vortices. Two possibilities have already been invented. One can either measure the magnetization field as in [16] or use Stern-Gerlach separation to measure the density of the different spin species.

Measuring the magnetization as a function of position is less informative for a *nonmagnetic* phase like the cyclic phase than for the ferromagnetic phase studied in Ref.

[16]. The magnetization outside the core of a vortex, where the spinor state is approximately a rotation of the unmagnetized cyclic state will be close to zero (see Eq. (45)), but inside the core, where the order parameter leaves the ground-state space  $\mathcal{M}$ , the magnetization can be nonzero. Measuring the magnetic moment in the core of a vortex helps to determine the topological charge of the vortex. (The magnetization will not provide any *direct* evidence of the rotating orientation of the tetrahedral order parameter, though.) Any vortex one might have to identify involves a rotation about an arbitrary axis  $\hat{\mathbf{n}}'$  as in Eq. (18), or Eq. (19) which is more convenient for understanding what a vortex will look like. The latter description starts with a vortex whose rotation axis is special—say it is parallel to  $\hat{\mathbf{z}}$ , and applies some overall rotation to it.

For example a vortex of type  $(R, \frac{2\pi}{3})$  can be obtained from a vortex whose axis is  $\hat{\mathbf{n}} = -\hat{\mathbf{z}}$ . Eq. (19) implies that the vortex is described by

$$\begin{aligned} \psi(r, \phi) &= D(R) e^{\frac{\xi}{3}(1+F_z)\phi} \sqrt{n_0} \left( f(r) \sqrt{\frac{1}{3}}, 0, 0, g(r) \sqrt{\frac{2}{3}}, 0 \right)^T \\ &= D(R) \sqrt{n_0} \left( f(r) e^{i\phi} \sqrt{\frac{1}{3}}, 0, 0, g(r) \sqrt{\frac{2}{3}}, 0 \right)^T, \end{aligned} \quad (88)$$

where  $f(r)$  and  $g(r)$  are appropriate functions approaching 1 at infinity and  $R$  is a rotation that moves  $\hat{\mathbf{n}} \rightarrow \hat{\mathbf{n}}'$ . (The phase,  $\xi$ , does not matter.) If  $\hat{\mathbf{n}}' = \hat{\mathbf{n}} = -\hat{\mathbf{z}}$ , then  $R$  is the identity, so  $m_x(r) = m_y(r) = 0$  and

$$\begin{aligned} m_z(r, \phi) &= \psi(r, \phi)^\dagger F_z \psi(r, \phi) \\ &= \frac{2}{3} [f(r)^2 - g(r)^2] n_0. \end{aligned} \quad (89)$$

The magnetization is parallel to the symmetry axis and is given by  $\mathbf{m} = \frac{2}{3} n_0 [g(r)^2 - f(r)^2] \hat{\mathbf{n}}$ . Applying an arbitrary reorientation  $R$  changes the magnetization axis and the symmetry axis in the same way, so the general result is

$$\mathbf{m} = \frac{2}{3} n_0 [g(r)^2 - f(r)^2] \hat{\mathbf{n}}'. \quad (90)$$

Far from the core, the magnetization vanishes. Inside the core, the magnetization can be found by noting that the top component of the vortex Eq. (88) must vanish at  $r = 0$  in order to be continuous:

$$f(0) = 0. \quad (91)$$

Since  $\alpha$  is much larger than  $\beta$  and  $\gamma$ , the density of atoms will be almost uniform across the whole vortex and hence  $\frac{1}{3} f(r)^2 + \frac{2}{3} g(r)^2 \approx 1$ . Eq. (91) therefore implies

$$g(0) \approx \sqrt{\frac{3}{2}}. \quad (92)$$

Hence the magnetization, Eq. (90), is approximately  $n_0 \hat{\mathbf{n}}'$  in the core; the atoms have a single unit of hyperfine spin in the direction of the vector from the center to the

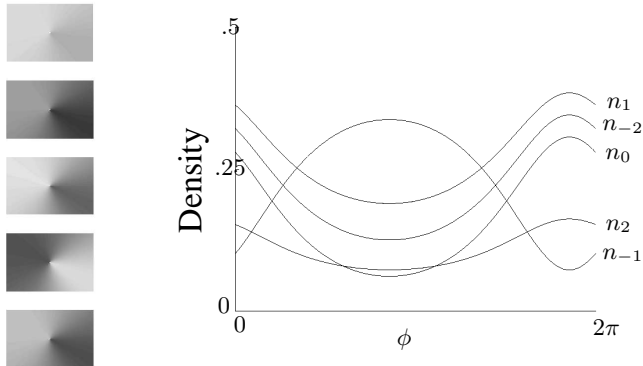


FIG. 9: Densities in the five spinor components around an order 3 vortex, with a randomly oriented local axis  $\hat{n}'$ . On the left is the pattern one might observe experimentally; the lighter regions correspond to regions with fewer atoms. On the right are plotted the percentage of atoms for each value of  $F_z$  at some fixed distance from the vortex core. The phases and amplitudes of these oscillations should help to determine the direction of the local axis.

*fixed* vertex of the rotating tetrahedra near vortex the core[57]. The inverse vortex,  $(R^{-1}, -\frac{2\pi}{3})$ , has the same magnetization (it does not change sign). On the other hand, similar arguments show that  $(R, -\frac{4\pi}{3})$  will have a magnetization approximately equal to  $-2n_0\hat{n}$  at the core center because it is the  $m = -1$  component of the spinor in the analogue of Eq. (88) that has the phase winding for this case. The third stable vortex type,  $(A, 0)$ , will not have any magnetization in its center and would be hard to see using this method. Measuring the magnetization reveals vortices of order three but does not distinguish between vortices and antivortices and does not even indicate the presence of an order two vortex. (One *can* observe the composite vortex described in Section IV A.) Another deficiency is that the cores are only about  $1 \mu\text{m}$  across, so the vortices might be hard to observe directly by this method. However, one could first allow the condensate to expand in the transverse direction so that the atomic interactions decrease. The vortex cores would expand; as in experimental observations of vortices in single-component condensates, the depleted region in  $f$  or  $g$  (whichever corresponds to the component of the transformed spinor with the phase winding) would fly apart and the magnetized core would become much larger. A magnetized ring would form at the edge of the core where the atoms of one magnetization accumulate more than the atoms of the other.

The Stern-Gerlach method gives more information about the vortices. Though the density is depleted at the center, the field *around* a vortex in a single-component condensate is not observable, unless one reconstructs the phase variation of the condensate, perhaps using the technique described in Ref. [49]. But in a spinor condensate, the spin vortices produce observable patterns in the condensates' Stern-Gerlach images. These images capture separately the density of atoms in each of the

five components of the spinor as functions of position. In these density profiles each vortex (aside from pure phase vortices with  $g = id$ ) will be ornamented by radiating density ripples as illustrated in Fig. 9. For example, according to Eq. (88), the density of atoms with  $F_z = m$  is given by

$$\begin{aligned} \frac{n(r, \phi, m)}{n_0} &= |D_{m2}(R)\sqrt{\frac{1}{3}}f(r)e^{i\phi} + D_{m,-1}(R)\sqrt{\frac{2}{3}}g(r)|^2 \\ &= a_m + b_m \cos(\phi - \phi_m). \end{aligned} \quad (93)$$

where  $a_m, b_m$  are constants outside the vortex cores, since  $f(r)$  and  $g(r)$  approach 1. While a vortex in a condensate of a single type of atom does not show any density modulation (unless the condensate interferes with a second condensate, see e.g. Ref. [50]), angular density ripples do result for a spinor vortex as a result of the interference between the  $f$  and  $g$  components of the spinor produced by of the unitary transformation changing the quantization axis from the vortex's rotation axis  $\hat{n}'$  to the magnetic field direction. If the  $\hat{n}'$  axis happens to line up exactly with the axis of the Stern-Gerlach field, then there are no radial "interference fringes," but only the axes of *point* vortices with aligned charges will tend to line up with  $\mathbf{B}$ . This is illustrated by the qualitative wave function in Section III. (See Eqs. (61), (62).)

Both the order three and order two vortices will be visible based on the images of the five spin components. One can determine the types of the vortices and their axes  $\hat{n}'$  (which are encoded in  $D(R)$ ) from the average magnitude of the densities  $a_m$  together with the amplitudes  $b_m$  and offsets  $\phi_m$  of the density modulations. (An order 2 vortex will have  $\cos 2\phi$  and  $\sin 2\phi$  Fourier modes in addition to the terms given in Eq. (93).) A possible difficulty with this method arises because, once the five spin components are separated in space, the density oscillations in each of them are no longer stable. The ensuing dynamics in the clouds could mix the atoms up.

Distinguishing among vortices with the same rotation but different phase winding numbers  $\theta$  is not possible with this method without resolving the cores. For example, the vortices  $(R, \frac{2\pi}{3})$  and  $(R, -\frac{4\pi}{3})$  have the same density patterns, since they differ only by an overall phase  $e^{i\phi}$ .

One would also hope to check some predictions about the size and charges of the bound states. One can select clusters of vortices in an image of the condensate (if there are not too many vortices) and use the methods just discussed to identify the vortex charges and check that each cluster satisfies Eq. (54). Additionally, a sign that the vortex clusters are actually *bound* states is that the bound state size depends in the right way on the magnetic field. Now atoms whose ground state is cyclic may be difficult to find ( $^{87}\text{Rb}$  is likely to be polar[39], though it may be possible to adjust the interaction parameters by applying light fields.). The general considerations of this article also apply to spin 3 condensates (see Ref. [51]), as well as to spin 1 condensates and pseudospin  $\frac{1}{2}$

condensates as already studied by [11, 12]. So we will estimate the bound state sizes for the more generic phases as well as for the cyclic phase. The cyclic phase is unique because the misalignment energy is a second order effect (see Sec. II A). For other phases where the misalignment energy is a first order effect of the Zeeman energy, the effective potential would be on the order of  $qn_0$ . Hence

$$L_q \sim \frac{\hbar}{\sqrt{mq}} \text{ for phases with } V_{eff} \propto q. \quad (94)$$

In contrast, for the cyclic phase, Eq. (66) can be expressed in terms of the scattering lengths as

$$L_q \sim \sqrt{n_0 \Delta a} \frac{\hbar^2}{mq} \text{ for cyclic phase} \quad (95)$$

Since  $q = \frac{\mu_B^2 B^2}{8A_{HF}}$ , the size of the molecules in the cyclic phase is proportional to  $\frac{1}{B^2}$  and the size of molecules in phases with  $V_{eff} \propto q$  is proportional to  $\frac{1}{B}$ .

The size of the condensate must be large enough hold an entire vortex molecule. Substituting  $B_{Max}$  from Eq. (87) into Eqs. (94) and (95) one finds that  $L_q(B_{Max}) \sim \frac{1}{\sqrt{\Delta a n_0}} \sim a_c$  (for either phase). This size is the magnetic healing length of the condensates (and the size of a vortex core) and is on the order of  $1 \mu\text{m}$ . The condensate should be narrow in one direction (so that the behavior of the order parameter is two-dimensional) but at least several times wider than the magnetic healing length in the other two directions; in order to measure the field dependence of the molecule sizes, one should be able to decrease the magnetic field by some factor below  $B_{Max}$  without the molecules leaving the condensate.

As a side-comment, vortex molecules probably undergo transitions at fields close to  $B_{Max}$  (see Fig. 10) since the component vortices overlap at larger fields. Absolutely stable vortex molecules, like example 3 in Table I, will be compressed so that the cores coincide and the vortex becomes rotationally symmetric at a finite field. Once the components' cores overlap a little bit, being slightly offset might not lead to significant savings in kinetic energy. On the other hand, when the vortices in a *metastable* molecule are squeezed together, they form an unstable tetrahedral vortex. Metastability occurs only when the ‘‘Coulomb’’ force keeps the component vortices apart.

## VI. CONCLUSION

We have shown that vortex molecules can be understood reasonably well based only on simple group theory and rough energy estimates. Some of these vortex molecules are actually metastable, and we can study their possible break-up ‘‘channels,’’ reminiscent of some of the decay processes in nuclear physics. (In practice, the molecules will probably escape through the surface of the condensate before any kind of ‘‘ultracold fusion’’ can happen!)

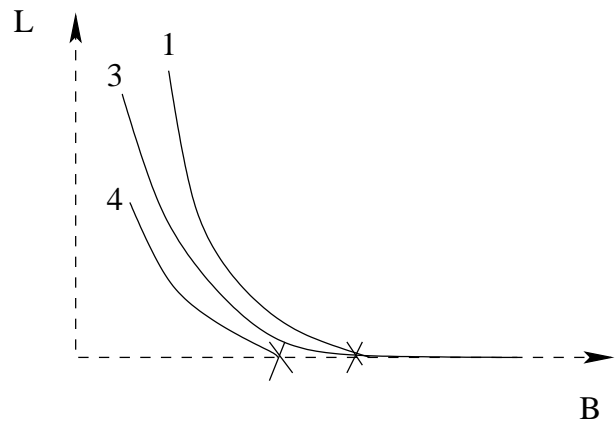


FIG. 10: The evolution of vortex molecules as the magnetic field is increased. The three curves illustrate how the sizes of the molecules from Table I, for  $c > 4$ , might change as the strength of the magnetic field is increased. The sizes decrease as  $\frac{1}{B^2}$ . At a certain magnetic field, an absolutely stable vortex will become rotationally symmetric and the component cores will coincide (molecule 3). Metastable vortices will become unstable when a certain magnetic field is reached, indicated by the x’s terminating the curves corresponding to molecules 1 and 4.

More accurate calculations of the vortex fields and energies could address other interesting questions. As is well-known, unlike the Coulomb interaction between vortices in an ordinary scalar superfluid, the interaction energy cannot be written as a sum of two-vortex interaction terms, as indicated by our estimate in terms of the energy index. A more accurate understanding of the kinetic energy landscape might show that the vortices in a molecule can have several spatial arrangements in the core. Another problem that requires more detailed calculations of vortex fields is determining whether a vortex with charge  $(R, -\frac{4\pi}{3})$  is stable: the energy index estimate shows that it can break up into vortices with only a finite change in energy, but whether the energy *increases* or *decreases* is not clear yet.

*Acknowledgments* We wish to thank R. Barnett, M. Greiner, H. Y. Kee, J. Moore, K. Sengstock, D. Stamper-Kurn, and W. P. Wong for useful conversations. We also acknowledge financial support from CUA, DARPA, MURI, AFOSR and NSF grant 0705472.

## APPENDIX A: APPENDIX: FINDING THE EFFECTIVE ACTION

Eq. (39) is not as difficult to minimize as it appears, because of the special symmetry of  $\chi_2$ . We must substitute  $\tilde{\psi} = \sqrt{n_0} \chi_2 + \delta\tilde{\psi}$ , where

$$\delta\tilde{\psi} = d\chi_2 + aF_x\chi_2 + bF_y\chi_2 + cF_z\chi_2 + (e + if)\chi_{2t} \quad (A1)$$

into the energy, Eq. (39). The perturbation  $\delta\tilde{\psi}$  is the deformation of the tetrahedron, measured relative to its

body axes. Let us figure out how many powers of the coefficients  $a, b, \dots$  to keep at each stage of calculating  $V$ . It helps to complete the square in Eq. (39) to get

$$V_{tot}(\psi) = \frac{1}{2}\alpha(\tilde{\psi}^\dagger\tilde{\psi} - n_0)^2 + \frac{1}{2}\beta(\tilde{\psi}^\dagger\mathbf{F}\tilde{\psi})^2 + \frac{1}{2}\gamma|\tilde{\psi}_t^\dagger\tilde{\psi}|^2 - \frac{1}{2}\alpha n_0^2 - q \sum_{i,j=1}^3 \cos\alpha_i \cos\alpha_j \tilde{\psi}^\dagger F_i F_j \tilde{\psi}, \quad (\text{A2})$$

where we note that the chemical potential for the cyclic state is  $\mu = \alpha n_0$  and define  $\gamma = c\beta$ . We also use  $F_{1,2,3}$  to stand for  $F_{x,y,z}$ . We need to find the minimum of this energy only to quadratic order in  $q$ . At the end we will find that  $a, b, c, \dots$  are each *linear* in  $q$ . Since each of the squared quantities in  $V$  vanishes when  $a, b, c, \dots = 0$ , just the linear contributions from  $a, b, c, \dots$  give the potential to quadratic order in  $q$ . The quadratic Zeeman term, since it is multiplied by  $q$ , also is not needed beyond linear order in  $a, b, c, d, e, f$ .

Next find which matrix elements of  $\chi_2$  need to be calculated to evaluate all these contributions to the energy. Only the cross terms between the unperturbed part  $\sqrt{n_0}\chi_2$  and the perturbation give linear functions of  $a, b, c, d, e, f$ . For example, one cross-term contained in the quadratic Zeeman contribution is

$$\tilde{\psi}^\dagger F_x F_y \tilde{\psi} \approx n_0 \chi_2^\dagger F_x F_y \chi_2 + 2\sqrt{n_0} \Re \chi_2^\dagger F_x F_y [(aF_x + bF_y + cF_z + d)\chi_2 + (e + if)\chi_{2t}]. \quad (\text{A3})$$

Expanding this gives a sum of matrix elements such as  $\chi_2^\dagger F_x F_y \chi_2$  and  $\chi_{2t}^\dagger F_x F_y F_z \chi_2$ . We need only the matrix elements of products of at most three  $F$ 's. Many of these (e.g.,  $\chi_2^\dagger F_i F_j F_k \chi_2$  when  $i, j, k$  are not all different, and  $\chi_{2t}^\dagger F_i F_j \chi_2$  when  $i$  and  $j$  are different) are equal to zero because of the 180° symmetries of  $\chi_2$  around the coordinate axes. The numerical values of the few remaining ones can be worked out quickly. Using these matrix elements to calculate all the terms in Eq. (A2) produces an expression  $V_{tot}(a, b, c, d, e, f, \cos\alpha_1, \cos\alpha_2, \cos\alpha_3)$ . Along the way, one notices that each of the variables  $a, b, c, \dots$  contributes to only one term in the  $q = 0$  potential (the first line of Eq. (A2)). The variables  $a, b, c$  determine the magnetization,  $d$  determines the density perturbation and  $e$  and  $f$  determine the singlet-amplitude  $\theta$ . E.g.,

$$\begin{aligned} n &= n_0 + 2\sqrt{n_0}d \\ M_x &= 4\sqrt{n_0}a \\ \Re[\theta] &= 2\sqrt{n_0}e. \end{aligned} \quad (\text{A4})$$

Finally, minimize the potential. It can be written as a sum of independent quadratic functions of  $a, b, c, d, e,$

and  $f$ :

$$\begin{aligned} V &= \left(-\frac{1}{2}\alpha n_0^2 + 2qn_0\right) + 2\alpha n_0 d^2 - 4\sqrt{n_0}qd \\ &\quad + 8\beta n_0(a^2 + b^2 + c^2) + 4\sqrt{3n_0}q(a \cos\alpha_2 \cos\alpha_3 \\ &\quad \quad + b \cos\alpha_1 \cos\alpha_3 + c \cos\alpha_1 \cos\alpha_2) \\ &\quad + 2\gamma n_0(e^2 + f^2) \\ &\quad + 2q\sqrt{n_0}[e(\cos^2\alpha_1 + \cos^2\alpha_2 - 2\cos^2\alpha_3) \\ &\quad \quad + \sqrt{3}f(\cos^2\alpha_1 - \cos^2\alpha_2)]. \end{aligned} \quad (\text{A5})$$

(Note that the second term,  $2qn_0$ , is the first-order contribution of the Zeeman energy, which is independent of orientation.)

Minimizing each quadratic (which gives  $a = -\frac{\sqrt{3}q}{4\beta\sqrt{n_0}} \cos\alpha_2 \cos\alpha_3, \dots$ ) and combining the results together with the help of Eq. (37) gives

$$\begin{aligned} V_{eff} &= -\frac{1}{2}\alpha n_0^2 + 2qn_0 - 2\frac{q^2}{\alpha} + \frac{q^2}{\gamma} - \frac{3q^2}{4\beta} \\ &\quad + \left(\frac{3q^2}{4\beta} - \frac{3q^2}{\gamma}\right)(\cos\alpha_1^4 + \cos\alpha_2^4 + \cos\alpha_3^4); \end{aligned} \quad (\text{A6})$$

all the constant terms can be dropped to give Eq. (4). Note that the magnetization varies with the orientation of the tetrahedron (as can be checked by substituting the optimal values for  $a, b, c$  into the magnetization, Eq. (A4)). In particular, the  $c > 4$  ground state with  $\cos\alpha_1, \cos\alpha_2, \cos\alpha_3 = \pm\frac{1}{\sqrt{3}}$  has a small magnetization,  $\mathbf{m} = \mp\frac{q}{\beta\sqrt{3}}(1, 1, 1)$ ; since this has been calculated from  $\tilde{\psi}$ , it is the magnetization *relative to the body axes* tetrahedron. Comparing this to the magnetic field relative to the body axes,  $B(\cos\alpha_1, \cos\alpha_2, \cos\alpha_3) = \frac{B}{\sqrt{3}}(1, 1, 1)$ , shows that the state will become magnetized either parallel or antiparallel to the magnetic field.

The point of the effective potential is that it allows us to eliminate the 6 most rigid degrees of freedom corresponding to  $a, b, c, d, e,$  and  $f$ ; then it is easier to understand vortex textures by concentrating on the rephasing and rotation angles as a function of position. The wavefunction in Eq. (11) can be parameterized in terms of Euler angles for the rotation, e.g.,  $\psi = \sqrt{n_0}e^{i\sigma F_z} e^{i\tau F_x} e^{i\rho F_z} e^{i\theta} \chi_2$ . The first angle,  $\sigma$ , does not come into the angles  $\alpha_i$  that describe the orientation of the magnetic field ( $B\hat{\mathbf{z}}$ ) relative to the tetrahedron. (The tetrahedron can be rotated around the  $z$ -axis without changing these angles.) One can check that  $\cos\alpha_1 = \sin\tau \sin\rho$ ,  $\cos\alpha_2 = -\sin\tau \cos\rho$ , and  $\cos\alpha_3 = \cos\tau$ . Now, working out the kinetic energy and combining it with the effective potential gives the “phase-and-



rotation-only” energy functional

$$\begin{aligned} \mathcal{E}_{eff} = & \iint d^2\mathbf{r} \frac{n_0 \hbar^2}{2m} [2(\nabla\rho)^2 + 2(\nabla\tau)^2 + 2(\nabla\sigma)^2 + \\ & (\nabla\theta)^2 + 4\cos\tau\nabla\sigma \cdot \nabla\rho] \\ & + (c-4)\frac{3q^2}{4c\beta} [\cos^4\tau + \sin^4\tau(\sin^4\rho + \cos^4\rho)]. \end{aligned} \quad (\text{A7})$$

This can be solved (in principle) to give the textures around sets of vortices and the relative positions of the vortices in equilibrium. Each vortex type implies a certain type of discontinuity in the four angles as the core is encircled. This expression does not seem too easy to use, but at least it shows just the two effects we have been balancing against one another (kinetic and anisotropy energy). The size of a vortex molecule can be estimated by assuming that the two terms are comparable,  $\frac{n_0 \hbar^2}{mL_q^2} \sim |c-4|\frac{q^2}{c\beta}$ . If distances are rescaled by  $L_q$ , we then find that the energy function has a form that depends only on the *sign* of  $c-4$ . Therefore, in a molecule with three vortices, the angles of the triangle they form will be independent of all the parameters, including  $c$ , even though it is dimensionless.

Eq. (A7) is derived from Eq. (32) by determining how the tetrahedra are distorted by the quadratic Zeeman effect. But the kinetic energy also causes distortions of the wave function from the perfect tetrahedral forms, and it seems possible that these distortions could lead to kinetic effects in the anisotropy term and anisotropy effects in the kinetic energy term. However, at the lowest order, treating the two terms independently seems correct. A simple argument for this (neglecting the kinetic energy when finding the anisotropy potential) is that the distortion due to the Zeeman term is linear in  $q$  while the distortion due to the kinetic energy is quadratic in  $q$ . To see this, think of an ordinary scalar vortex, where the density varies as  $n_0(1 - \frac{a^2}{r^2})$  far from the core[2]. The amount of “distortion” is  $-\frac{a^2}{r^2}n_0$ . In the cyclic state, distortion (i.e., perturbations to the spinor components that take it out of  $\mathcal{M}$ ) implies changes in the magnetization as well as the density. But we may assume that these distortions are still of order  $\frac{a^2}{r^2}n_0$ . The majority of the “pulp” in a molecule’s core consists of points whose distance is of order  $L_q$  from the actual vortex cores (the “seeds”), so the amount of distortion can be found by substituting  $r = L_q$  from Eq. (10). Using the relation between  $a_c$  and  $\beta$  shows that the fractional distortion in the “pulp” regions is of order  $\frac{a^2}{r^2}n_0 \sim (\frac{q}{n_0\beta})^2$ , to be compared with the deformations of order  $\frac{q}{\beta n_0}$  that result from minimizing Eq. (A5).

## APPENDIX B: APPENDIX: NONCOMMUTATIVITY OF VORTEX CHARGES

To give a complete description of charge conservation when the charges are described by the noncommuting rotations of a tetrahedron, one needs to give a rule for how to multiply the charges of a set of vortices together to get the net charge. A convention we used is to multiply the topological charges together in order of increasing x-coordinates.

It seems that this definition has an awkward consequence: does the net vortex charge jump suddenly when two of the vortices are reordered, because of the non-commutativity of the group of charges? In Fig. 11 vortices 1 and 2 are interchanged between frames a) and c), which suggests that the net charge changes from  $\Gamma_3\Gamma_2\Gamma_1$  to  $\Gamma_3\Gamma_1\Gamma_2$ . But this deduction is incorrect, and the net vortex charge *is* actually conserved.

The resolution of the paradox has to do with the fact that the charge of a vortex can only be determined up to conjugacy, unless one introduces a systematic convention. For example, the charge of a  $120^\circ$ -rotation vortex is ambiguous—the rotation could be either  $P$ ,  $Q$ ,  $R$ , or  $S$ , and there is no way to distinguish between these because the four vertices of the tetrahedra are indistinguishable. (Abstractly speaking, the four rotations are conjugate elements of the group.) In order to identify the charge of each vortex, we have to choose a routine for labelling the vertices of the tetrahedra nearby. Here is a convention that is consistent with the rule for ordering the vortex charges. Take a point  $O$  far below all the vortices in the system and connect it with lines to points just below the vortices (see Fig. 11a). Now identify the *base* tetrahedron at  $O$  with the standard tetrahedron in Fig. 2a, making a choice from among the twelve possible ways. The labelling at  $O$  can be communicated to the tetrahedron at the end-point of each line, by copying the labelling from  $O$  to a nearby tetrahedron on the line, and then continuing to copy the labelling until the end of the line is reached. Now the charges of the vortices can be identified by using the labelling of the nearby tetrahedron to assign a letter to the rotation axis.

Now that we have a consistent convention for assigning vortex charges, we can show that the net charge of a set of vortices does not change when two of them are interchanged. The trick is that the charges of the *individual* vortices do change in such a way that the product charge does not change! Between Fig. 11a and Fig. 11c, vortex 2 is moved over vortex 1. Because vortex 2’s tether gets tangled up with vortex 1 when vortex 1 passes below it, its charge gets redefined, as  $\Gamma_1^{-1}\Gamma_2\Gamma_1$ . The other two vortices’ charges do not change. The net charge, obtained by multiplying the vortex charges from left to right, is

$$\Gamma_3\Gamma_1(\Gamma_1^{-1}\Gamma_2\Gamma_1) = \Gamma_3\Gamma_2\Gamma_1.$$

Thus the net charge does not change. On the other hand, there is a sudden jump in the charge of vortex 2, but this does not mean that the fields of tetrahedra are changing

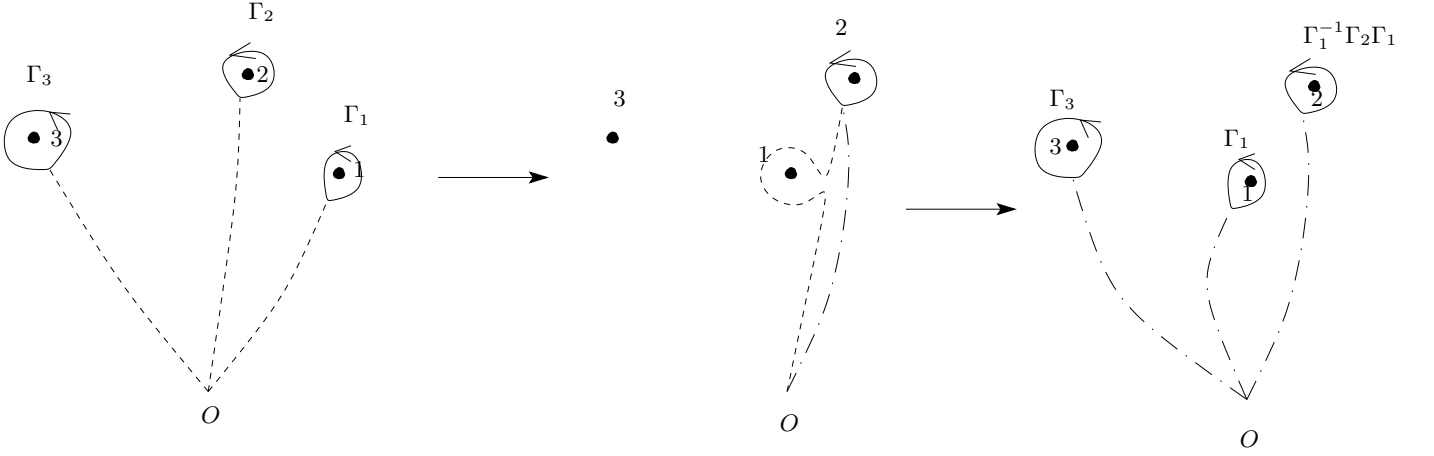


FIG. 11: a) The convention for assigning vortex charges. For a set of vortices, tethers are drawn directly from the origin to an anchor just below each vortex. As long as the tethers are moved continuously, the correspondence between the tetrahedral state at the anchor and the standard tetrahedral state does not change. b,c) These show what happens when vortex 1 is moved below vortex 2. The dashed lines in a) and the dash-dot-dash lines in c) are the tethers before and after vortex 1 moves. Part b) focuses on the tether of vortex 2, showing how the original tether gets pushed to the side by vortex 1 and is replaced by a new tether. Continuing the labelling of the tetrahedron vertices around the original path changes the labelling of the tetrahedron just below vortex 2. Hence the charge of vortex 2 is identified differently in c).

suddenly; the vortex has just been reclassified, with a vortex charge that is conjugate to the original charge.

Here is an interesting consequence of the noncommuting charges: the force between a pair of vortices changes from repulsive to attractive if a third vortex wanders between them. In Fig. 12 one vortex (the  $P$  one) catalyzes a reaction without touching the other two vortices involved. (Assume the phases are 0 for the two  $B$  vortices and  $\frac{2\pi}{3}$  for the  $P$  vortex.) To figure out what happens, keep track of when a vortex's connection to the reference point (below the figure) is interrupted by another vortex. The charge of the vortex passing underneath is not changed, and the charge of the vortex on top changes to keep the total charge the same. This information is sufficient for working out all the charges: When  $P$  passes below the  $B$  on the right, the latter vortex changes to a  $B' = P^{-1}BP$ , so that the net charge is still the same, even though  $P$  has moved. (This can be used to work out the charges: the net charge of the two vortices which have switched has to be the same, so  $PB' = BP$  so  $B' = P^{-1}BP$ .) Next, when  $P$  passes *above* the  $B$  on the left, the *former* vortex changes to a  $BPB^{-1}$  vortex. Now the  $SU_2$  matrices for  $B$  and  $P$  are  $-i\sigma_y$  and  $\frac{1-i\sigma_x+i\sigma_y+i\sigma_z}{2}$  (using the axes associated with  $\chi_2$ ). Multiplying out the charges shows that  $B' = A^{-1}$ . The force between the original pair of vortices (say the  $P$  is far away at the beginning and end) is  $\frac{n_0\hbar^2\pi}{mL}(I_E(B^2, 0) - I_E(B, 0) - I_E(B, 0))$  and the force between the vortices they turn into is

$\frac{n_0\hbar^2\pi}{mL}(I_E(BA^{-1}), 0) - I_E(A^{-1}, 0) - I_E(B, 0)$ . ( $L$  is the distance between the vortices.) The vortices repel each other at first, but after  $P$ 's intervention, they attract each other, as one sees by checking that  $BA^{-1} = C$ , and that  $B^2$  is a  $2\pi$  rotation with energy index 2 while the other

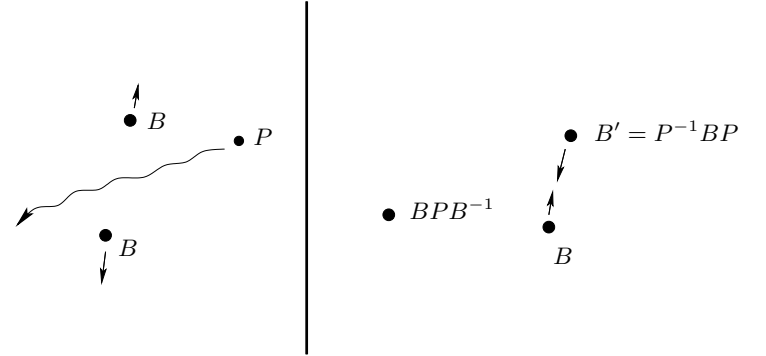


FIG. 12: Catalysis by conjugation; the vortex on the right moves between the other two vortices changing their repulsion to attraction.

reacting charges are all  $\pi$  rotations, with index  $\frac{1}{2}$ .

We have been assuming that  $q = 0$ , but a similar reaction could also happen in the core of a composite vortex when  $q \neq 0$ ; that is why one has to check all the possible ways for vortices to wander between one another before coalescing or before dividing into groups.

[1] S. Chandrasekhar (1994).

[2] C. J. Pethick and H. Smith, *Bose-Einstein Condensa-*

- tion in Dilute Gases* (Cambridge University Press, Cambridge, 2002).
- [3] L. P. Pitaevskii and S. Stringari, *Bose-Einstein condensation* (Clarendon Press, Oxford, 2003).
  - [4] J. Stenger, S. Inouye, D. Stamper-Kurn, H.-J. Miesner, A. Chikkatur, and W. Ketterle, *Nature* **396**, 345 (1998).
  - [5] T.-L. Ho, *Physical Review Letters* **351**, 742 (1998).
  - [6] T. Ohmi and K. Machida, *Journal of the Physical Society of Japan* **67**, 1822 (1998).
  - [7] M. Lewenstein, A. Sanpera, V. Ahufinger, B. Damski, A. S. De, and U. Sen, *Advances in Physics* **56**, 243 (2007).
  - [8] I. Bloch, *Journal of Physics B* **38**, S629 (2005).
  - [9] C. Ciobanu, S.-K. Yip, and T.-L. Ho, *Physical Review Letters* **61**, 033607 (2000).
  - [10] N. D. Mermin, *Reviews of Modern Physics* **51**, 591 (1979).
  - [11] K. Kasamatsu, M. Tsubota, and M. Ueda, *Physical Review Letters* **93**, 250406 (2004).
  - [12] T. Isoshima and S. Yip, *Journal of the Physical Society of Japan* **75**, 074805 (2006).
  - [13] H. Makela and K. A. Suominen, *Physical Review Letters* **99**, 190408 (2007).
  - [14] C. Wu, *Modern Physics Letters B* **20**, 1707 (2006).
  - [15] D. Controzzi and A. M. Tsvelik, *Physical Review Letters* **96**, 097205 (2006).
  - [16] L. E. Sadler, J. M. Higbie, S. R. Leslie, M. Vengalattore, and D. M. S. Kurn, *Nature* **443**, 7109 (2006).
  - [17] I. Chuang, R. Durrer, N. Turok, and B. Yurke, *Science* **251**, 4999 (1991).
  - [18] V. Pietila, M. Mottonen, T. Isoshima, J. A. M. Huhtamaki, and S. M. M. Virtanen, *Physical Review A* **74**, 023603 (2006).
  - [19] M. Uhlmann, R. Schützhold, and U. R. Fischer, *Physical Review Letters* p. 120407 (2007).
  - [20] A. Lamacraft, *Physical Review Letters* **98**, 160404 (2007).
  - [21] R. W. Cherg, V. Gritsev, D. M. Stamper-Kurn, and E. Demler, *Physical Review Letters* **100**, 180404 (2008).
  - [22] A. Lamacraft, *Physical Review A* **77**, 063622 (2008).
  - [23] M. Moreno-Cardoner, J. Mur-Petit, M. Guilleumas, A. Polls, A. Sanpera, and M. Lewenstein, *Physical Review Letters* **99**, 020404 (2007).
  - [24] M. Vengalattore, S. R. Leslie, J. Guzman, and D. M. Stamper-Kurn, *Physical Review Letters* **100** (2008).
  - [25] K. Gross, C. P. Search, H. Pu, W. Zhang, and P. Meystre, *Physical Review A* **66**, 033603 (2002).
  - [26] R. Barnett, S. Mukerjee, and J. E. Moore (2007), arXiv:0710.5550.
  - [27] K. Kasamatsu, M. Tsubota, and M. Ueda, *International Journal of Modern Physics B* **19**, 1835 (2005).
  - [28] A. E. Leanhardt, A. Gorlitz, A. P. Chikkatur, D. Kielpinski, Y. Shin, D. E. Pritchard, and W. Ketterle, *Physical Review Letters* **89**, 190403 (2002).
  - [29] A. E. Leanhardt, Y. Shin, D. Kielpinski, D. E. Pritchard, and W. Ketterle, *Physical Review Letters* **90**, 140403 (2003).
  - [30] Y. Shin, M. Saba, M. Vengalattore, T. A. Pasquini, C. Sanner, A. E. Leanhardt, M. Prentiss, D. E. Pritchard, and W. Ketterle, *Physical Review Letters* **93**, 160406 (2004).
  - [31] U. A. Khawaja and H. T. C. Stoof, *Physical Review A* p. 043612 (2001).
  - [32] H. Zhai, W. Chen, Z. Xu, and L. Chang, *Physical Review A* **68**, 043602 (2003).
  - [33] H. Stoof, E. Vliegen, and U. A. Khawaja, *Physical Review Letters* **87**, 120407 (2001).
  - [34] Y. Kawaguchi, M. Nitta, and M. Ueda, *Physical Review Letters* **100**, 180403 (2008).
  - [35] Y. Zhang, H. Mäkelä, and K. Suominen, *Chinese Physics Letters* **22**, 536 (2005), see also arxiv:cond-mat/0305489.
  - [36] R. Barnett, A. Turner, and E. Demler, *Physical Review Letters* **97**, 180412 (2006).
  - [37] R. Barnett, A. Turner, and E. Demler, *Physical Review A* **76**, 013605 (2007).
  - [38] J. Kronjager, C. Becker, P. Navez, K. Bongs, and K. Sengstock, *Phys. Rev. Lett.* **97**, 110404 (2006).
  - [39] M.-S. Chang, C. D. Hamley, M. D. Barrett, J. A. Sauer, K. M. Fortier, W. Zhang, L. You, and M. S. Chapman, *Physical Review Letters* **92**, 140403 (2004).
  - [40] A. Widera, F. Gerbier, S. Fölling, T. Gericke, O. Mandel, and I. Bloch, *New Journal of Physics* **8**, 152 (2006).
  - [41] H. Schmaljohann, M. Erhard, J. Kronjäger, M. Kottke, S. van Staa, L. Cacciapuoti, J. J. Arlt, K. Bongs, and K. Sengstock, *Physical Review Letters* p. 040402 (2004).
  - [42] D. M. Stamper-Kurn and W. Ketterle, in *Coherent atomic matter waves-Ondes de matiere coherentes (Les Houches LXXII)*, edited by R. Kaiser, C. Westbrook, and F. David (Springer, Berlin, 1999).
  - [43] D. R. Nelson, *Defects and Geometry in Condensed Matter Physics* (Cambridge University Press, Cambridge, 2002).
  - [44] Barnett, ryan Barnett, private communication.
  - [45] M. Ueda and M. Koashi, *Physical Review A* **65**, 063602 (2002).
  - [46] S. Chandrasekhar and G. S. Ranganath, *Advances in Physics* **35**, 507 (1986).
  - [47] M. F. Andersen, C. Ryu, P. Clade, V. Natarajan, A. Vaziri, K. Helmerson, and W. D. Phillips, *Physical Review Letters* **97**, 170406 (2006).
  - [48] T. Isoshima, K. Machida, and T. Ohmi, *Journal of the Physical Society of Japan* **70**, 1604 (2001).
  - [49] D. Meiser and P. Meystre, *Physical Review A* **72**, 023605 (2005).
  - [50] S. Stock, Z. Hadzibabic, B. Battelier, M. Cheneau, and J. Dalibard, *Physical Review Letters* **95**, 190403 (2005).
  - [51] A. Griesmaier, J. Werner, S. Hensler, J. Stuhler, and T. Pfau, *Phys. Rev. Lett.* **94**, 160401 (2005).
  - [52] This is a small oversimplification. Decreasing the size of the space  $\mathcal{M}$  also stabilizes vortices that would be unstable at  $q = 0$ —removing a portion of  $\mathcal{M}$  can leave a new hole for a vortex-circuit to wrap around.
  - [53] The  $\alpha$ 's for this vortex may be calculated by noting that, relative to the tetrahedron, the  $z$ -axis of space rotates  $180^\circ$  about  $A$  so that  $(\cos \alpha_1, \cos \alpha_2, \cos \alpha_3)$ , its coordinates relative to the body axes of the tetrahedron are easy to work out as functions of  $\phi$ .
  - [54] Hence, when  $c > 4$ , the fluid is ferromagnetic—i.e., it becomes spontaneously magnetized either parallel or antiparallel to the external magnetic field with an  $\mathbf{m}$  that can be calculated from the expressions in Appendix A. This magnetization spontaneously breaks a symmetry since the quadratic Zeeman effect is invariant under  $F_z \rightarrow -F_z$ . For zero net magnetization, domains will form that have magnetization in both directions. Even in the presence of a small cubic Zeeman term, one can show that there is a discontinuous phase transition (as the thermodynamical variable conjugate to magnetization is varied) although the symmetry between  $\pm \hat{z}$  is not exact.

[55] Using the equations, the quadratic Zeeman term distorts the ground state  $\sqrt{n_0}\chi_3$  with increasing magnetic field  $B$  into  $\psi_3(B) = \sqrt{n_0}(X(B), 0, 0, Y(B), 0)^T$  with  $X > \sqrt{\frac{1}{3}}, Y < \sqrt{\frac{2}{3}}$  because the quadratic Zeeman field favors large values of  $|F_z|$ . The ground state  $\sqrt{n_0}\chi_2$  distorts into  $\psi_2(B) = \sqrt{n_0}(X'(B), 0, -iY'(B), 0, X'(B))$  with  $X' > \frac{1}{2}$  and  $Y' < \frac{1}{\sqrt{2}}$ . The deformed state  $\psi_3(B)$  has a nonzero  $\mathbf{m}$  and a vanishing  $\theta$  and  $\psi_2(B)$  is the other way around. Incidentally, when  $B$  becomes large enough, the ground state will become more symmetrical, with  $X$  and  $X' = 1$  (compare with Ref. [26]).

[56] The break-up only lowers the net energy by a *finite* amount, about  $\pi \frac{n_0 \hbar^2}{m} \ln \sqrt{\frac{\alpha}{\beta}}$  and the fragments interact with a short-range repulsion,  $\propto \ln r/r^3$  perhaps; when the energy index of the fragments actually decreases the force is  $\propto \frac{1}{r}$ . Whether  $(R, -\frac{4\pi}{3})$  is stable or not we do not know, and the answer may depend on  $c$ .

[57] Hence, the direction of the magnetization,  $\hat{\mathbf{n}}$ , helps determine the orientation of the tetrahedra near each vortex core, in spite of Eq. (46). If there are several vortices nearby one can try to guess how the tetrahedron fields around them fit together.